ARTICLES
https://doi.org/10.1038/s41589-021-00932-1
nature chemical biology

Check for updates

Engineering CAR-T cells to activate small-molecule drugs in situ

Thomas J. Gardner[1,9], J. Peter Lee[2,3,9], Christopher M. Bourne[1,4], Dinali Wijewarnasuriya[5,6], Nihar Kinarivala[2], Keifer G. Kurtz[1,7], Broderick C. Corless[2,7], Megan M. Dacek[1,7], Aaron Y. Chang[6], George Mo[1], Kha M. Nguyen[2], Renier J. Brentjens[5,7], Derek S. Tan[2,3,7,8] ✉ and David A. Scheinberg[1,3,5,7] ✉

Chimeric antigen receptor (CAR)-T cells represent a major breakthrough in cancer therapy, wherein a patient's own T cells are engineered to recognize a tumor antigen, resulting in activation of a local cytotoxic immune response. However, CAR-T cell therapies are currently limited to the treatment of B cell cancers and their effectiveness is hindered by resistance from antigen-negative tumor cells, immunosuppression in the tumor microenvironment, eventual exhaustion of T cell immunologic functions and frequent severe toxicities. To overcome these problems, we have developed a novel class of CAR-T cells engineered to express an enzyme that activates a systemically administered small-molecule prodrug in situ at a tumor site. We show that these synthetic enzyme-armed killer (SEAKER) cells exhibit enhanced anticancer activity with small-molecule prodrugs, both in vitro and in vivo in mouse tumor models. This modular platform enables combined targeting of cellular and small-molecule therapies to treat cancers and potentially a variety of other diseases.

Targeted cellular therapies are a promising new approach to treat cancers and other human diseases[1–3]. These living therapeutics undergo logarithmic proliferation triggered by recognition of a target antigen, leading to high concentrations of the therapeutic cells at the disease site. Foremost among these are CAR-T cells, derived from a patient's own T cells and engineered to recognize tumor antigens and to kill via a cytolytic immune response. So far, five CAR-T cell therapies have been approved for treatment of B cell cancers[4]. Despite these breakthroughs, cellular therapies have several important limitations and lack efficacy in most other cancers, including solid tumors[5,6]. Even in the context of B cell malignancies, CAR-T cells cannot recognize antigen-negative cells, leading to incomplete therapeutic responses or later relapse[7–9]. Moreover, the immunologic functions of CAR-T cells can be suppressed by a variety of factors within the tumor microenvironment[10], resulting in dysfunctional or 'exhausted' T cells[11]. Finally, CAR-T cell treatment can result in life-threatening toxicities arising from the immune response itself[12].

To address these limitations, new generations of CAR-T cells with enhanced capabilities are being developed[13,14], such as 'armored' CAR-T cells engineered to release localized doses of therapeutic cytokines, immunostimulatory ligands or antibody fragments[15–19]. However, an approach that has not yet been explored is the development of CAR-T cells that can generate an orthogonally acting small-molecule drug locally at the disease site. This provides an attractive means to address the cancer resistance mechanisms described above, because a small-molecule drug with orthogonal anticancer activity would kill antigen-negative tumor cells, would not be hindered by the immunosuppressive tumor microenvironment or T cell exhaustion, could diffuse readily into the tumor mass providing broader efficacy beyond B cell neoplasms and may permit dose-sparing of the CAR-T cells to reduce the risk of toxicity arising from the immune response[20]. Further, local generation of the small-molecule drug at the tumor site would also reduce toxicity associated with systemic administration of the drug. While other approaches have been developed for antigen-targeted drug delivery, such as antibody–drug conjugates and antibody-directed enzyme–prodrug therapy (ADEPT)[21,22], the cell-based system envisioned here provides synergy with the CAR-T cell immune functions and also enables far higher levels of drug amplification, as the cells undergo logarithmic expansion at the disease site and each cell can, in turn, express thousands of copies of the enzymes that, in turn, generate the active drug catalytically. Bacterial delivery vectors for prodrug-activating enzymes have also advanced to the clinic, but lacked tumor antigen targeting and required intratumoral injection[23].

Herein we report demonstration of this concept with SEAKER (synthetic enzyme-armed killer) cells, CAR-T cells engineered to activate systemically administered, inactive prodrugs locally at tumor sites, resulting in enhanced anticancer activity in vitro and in vivo. The small-molecule drug provides activity against antigen-negative cells, is still generated by exhausted T cells, extends efficacy to a solid tumor model and allows lower doses of the CAR-T cells to be used. We demonstrate the modularity and scope of this platform in SEAKER systems comprising two different activating enzymes and three classes of small-molecule drugs.

[1]Molecular Pharmacology Program, Sloan Kettering Institute, Memorial Sloan Kettering Cancer Center, New York, NY, USA. [2]Chemical Biology Program, Sloan Kettering Institute, Memorial Sloan Kettering Cancer Center, New York, NY, USA. [3]Tri-Institutional PhD Program in Chemical Biology, Memorial Sloan Kettering Cancer Center, New York, NY, USA. [4]Immunology Program, Weill Cornell Graduate School of Medical Sciences, Memorial Sloan Kettering Cancer Center, New York, NY, USA. [5]Department of Medicine, Memorial Hospital, Memorial Sloan Kettering Cancer Center, New York, NY, USA. [6]BCMB Allied Program, Weill Cornell Graduate School of Medical Sciences, Memorial Sloan Kettering Cancer Center, New York, NY, USA. [7]Pharmacology Program, Weill Cornell Graduate School of Medical Sciences, Memorial Sloan Kettering Cancer Center, New York, NY, USA. [8]Tri-Institutional Research Program, Memorial Sloan Kettering Cancer Center, New York, NY, USA. [9]These authors contributed equally: Thomas J. Gardner, J. Peter Lee.
✉e-mail: tand@mskcc.org; scheinbd@mskcc.org

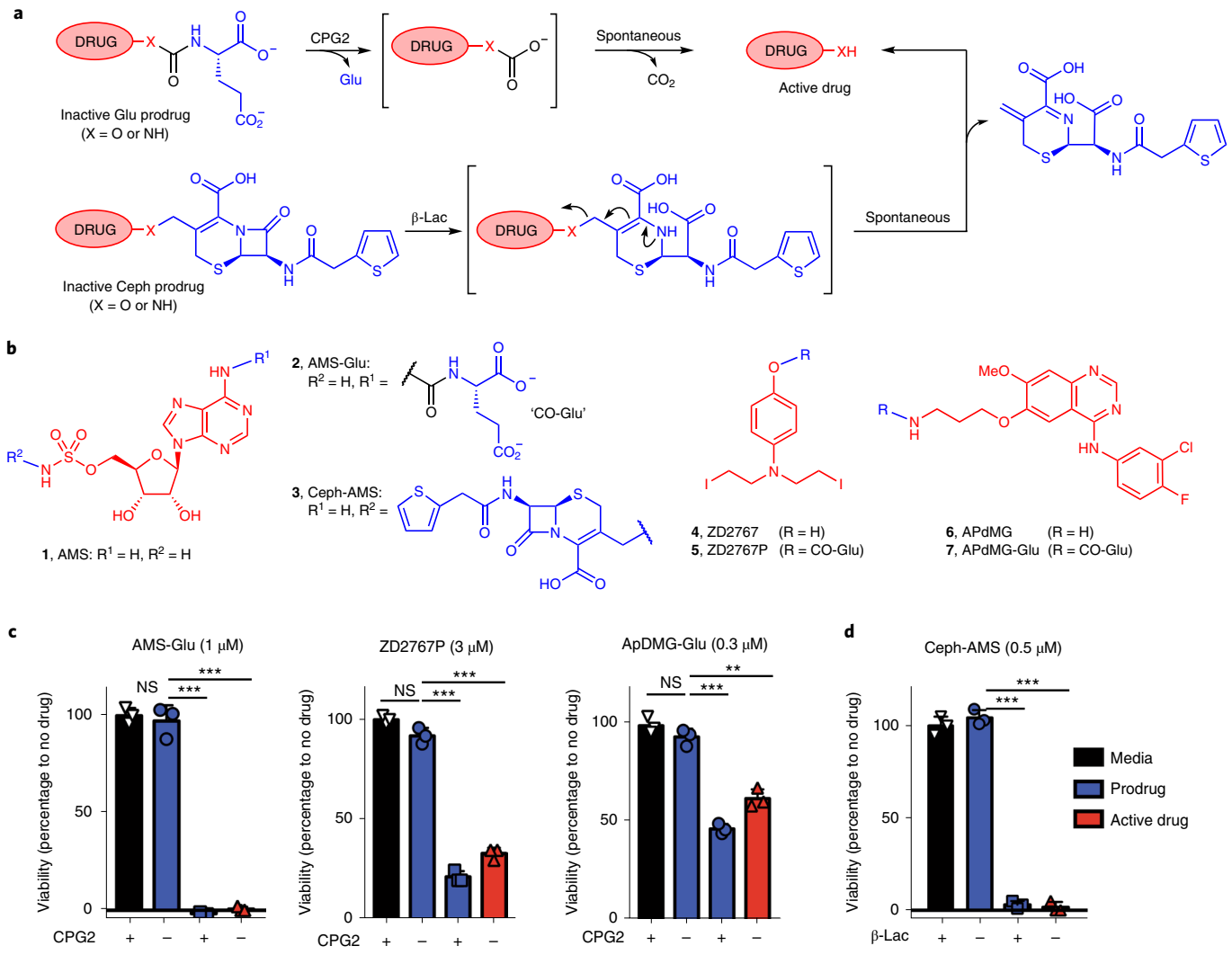

Fig. 1 | Modular prodrug designs for use with SEAKER cells. a, Glutamate-masked prodrugs can be cleaved with *Pseudomonas* sp. CPG2 to form a carbonic (X = O) or carbamic (X = NH) acid intermediate, followed by spontaneous decomposition of the linker to form the active drug. Cephalothin-masked prodrugs can be cleaved by *Enterobacter cloacae* β-Lac to form a hydrolyzed intermediate, followed by spontaneous elimination of the cephalothin byproduct to form the active drug. Drugs are shown in red, masks in blue, linkers in gray. **b**, Structures of cytotoxic natural product AMS (**1**), glutamate-masked prodrug AMS-Glu (**2**) and cephalothin-masked prodrug Ceph-AMS (**3**); nitrogen mustard ZD2767 (**4**) and glutamate-masked prodrug ZD2767P (**5**); and targeted kinase inhibitor APdMG (**6**) and glutamate-masked prodrug APdMG-Glu (**7**). (AMS, adenosine-5′-*O*-monosulfamate or 5′-*O*-sulfamoyladenosine; APdMG, 7-*O*-aminopropyl-7-*O*-des(morpholinopropyl)gefitinib). **c**, Cytotoxicity of prodrug AMS-Glu (**2**, 1 μM), ZD2767P (**5**, 3 μM), APdMG-Glu (**7**, 0.3 μM) (blue), with or without recombinant CPG2 (250 ng ml^{-1}), or of the parent drug AMS (**1**), ZD2767 (**4**), APdMG (**6**), respectively (red), to SET2 cells (48 h, CellTiter-Glo assay). **d**, Cytotoxicity of prodrug Ceph-AMS (**3**, 0.5 μM) (blue), with or without recombinant β-Lac (10 ng ml^{-1}), or of the parent drug AMS (**1**, 0.5 μM) (red) to SET2 cells (48 h, CellTiter-Glo assay). (For **c**,**d**, mean ± s.d. of $n = 3$ technical replicates; Student's two-tailed *t*-test: NS, not significant, $^{**}P < 0.01$, $^{***}P < 0.001$; representative of two or more experiments.)

Results

A wide range of enzymes and prodrugs can be considered for use in the SEAKER platform toward various therapeutic applications[22]. To demonstrate the feasibility and modularity of this approach, we developed two SEAKER systems that express different hydrolytic enzymes that can activate appropriately masked prodrugs, based on *Pseudomonas* sp. carboxypeptidase G2 (CPG2), which hydrolyzes C-terminal glutamate masking groups[24], and *Enterobacter cloacae* β-lactamase (β-Lac), which triggers cleavage of cephalosporin masking groups by hydrolysis of the β-lactam[25] (Fig. 1a). We selected these two enzymes to facilitate this first implementation of the SEAKER concept as they are well-characterized, having both been used previously in ADEPT systems. Notably, CPG2 constructs have advanced to human clinical trials in that context[22].

Design, synthesis and cytotoxicity of prodrugs. We designed four prodrugs for initial evaluation, using two different masking groups for cleavage by CPG2 or β-Lac and representing three different chemotypes and mechanisms of action (Fig. 1b). 5′-*O*-Sulfamoyladenosine (AMS, **1**) is a highly cytotoxic natural product[26,27] with a half-maximum inhibitory concentration (IC_{50}) of 1.77 nM in the NCI-60 Human Tumor Cell Lines Screen (NSC 133114). For use with CPG2 systems, the prodrug AMS-Glu (**2**) was designed with a glutamate masking group at the adenine 6-amino group of AMS, and synthesized in five steps from adenosine 2′,3′-*O*-acetonide (Extended Data Fig. 1) (see Supplementary Note for complete details). For β-Lac systems, the prodrug Ceph-AMS (**3**) was designed with a cephalothin masking group linked to the sulfamate nitrogen of AMS, and synthesized in seven steps from

adenosine (Extended Data Fig. 2). The nitrogen mustard ZD2767 (**4**) has been masked as a glutamate prodrug ZD2767P (**5**) that has advanced to human clinical trials in ADEPT[28], and was synthesized as previously described[29]. The parent drug **4** was synthesized in four steps from *O*-benzyl-4-aminophenol (Supplementary Fig. 1). Finally, APdMG (**6**, 7-*O*-aminopropyl-7-*O*-des(morpholinopropyl) gefitinib), an analogue of the targeted eGFP kinase inhibitor gefitinib, has been used in nanoparticle–drug conjugates[30] and the glutamate-masked prodrug APdMG-Glu (**7**) was synthesized in two steps from the known parent drug[30] (Supplementary Fig. 2).

We determined IC_{50} values for each prodrug–drug pair against a panel of cancer cell lines and primary cells to calculate selectivity indices (Supplementary Table 1). Selectivity indices ranged from roughly 1 log to >3 logs, with AMS-Glu (**2**) having the highest selectivities (556-fold median). All four prodrugs were deemed suitable for further evaluation.

Activation of prodrugs by recombinant enzymes. We first investigated whether these prodrugs would be accepted as substrates by the corresponding enzymes. Cleavage of the glutamate-masked prodrugs AMS-Glu (**2**), ZD2767P (**5**) and APdMG-Glu (**7**) by recombinant, purified CPG2 (Supplementary Fig. 3a) was evaluated using a glutamate release assay (Amplex Red), and all three prodrugs were accepted as substrates (Supplementary Fig. 3b). Cleavage of the cephalosporin-masked prodrug Ceph-AMS (**3**) was assessed using a recombinant, purified mutant of β-Lac reported to have reduced immunogenicity[31] (Supplementary Fig. 3c), and the prodrug was successfully converted to the parent drug AMS (**1**) (liquid chromatography–tandem mass spectrometry (LC–MS/MS) assay). Enzyme kinetic parameters were then determined using RapidFire solid-phase extraction/time-of-flight mass spectrometry (SPE–TOF–MS) assays (Supplementary Table 2).

Next, we tested whether the recombinant, purified enzymes would activate the cytotoxicity of the corresponding prodrugs against a SET2 leukemia cell line. The glutamate-masked prodrugs AMS-Glu (**2**), ZD2767P (**5**) and APdMG-Glu (**7**) all exhibited cytotoxicity in the presence of CPG2 comparable to that of the corresponding parent drugs, but were nontoxic alone (Fig. 1c). Moreover, AMS-Glu (**2**) was nontoxic to LNCaP prostate cancer cells that express human glutamate carboxypeptidase II (PSMA, prostate-specific membrane antigen) (Supplementary Fig. 4), consistent with stability of the glutamate mask to this endogenous enzyme. The cephalosporin-masked prodrug Ceph-AMS (**3**) also exhibited analogous cytotoxicity to SET2 cells in the presence of β-Lac (Fig. 1d). Based on their potent cytotoxicity and high selectivity indices (Supplementary Table 1), we selected AMS-Glu (**2**) and Ceph-AMS (**3**) for further investigations.

Activation of prodrugs by enzyme-expressing cells. We next sought to determine whether the AMS-Glu (**2**) and Ceph-AMS (**3**) prodrugs could be activated by mammalian cells expressing CPG2 or β-Lac, respectively. This required that these bacterial enzymes be expressed by the mammalian cells in active form and without harming the producing cells. Our initial efforts focused on AMS-Glu (**2**) and CPG2, and we designed both secreted (CPG2-sec) and membrane-anchored (CPG2-tm) forms of the enzyme to compare their effectiveness. We anticipated that the secreted form would provide higher local enzyme concentrations, but also that enzyme diffusion in vivo might result in off-tumor toxicity. In contrast, the membrane-anchored form could provide enzyme activity more tightly localized to the producing cells, but its expression and activity might be hindered by proximity to the lipid bilayer or other membrane proteins.

Initial experiments were carried out in human embryonic kidney 293T (HEK293T) cells by retroviral transduction with the CPG2 gene cassettes (Fig. 2a). The eukaryote-optimized CPG2 construct included two point mutations to prevent N-linked glycosylation[32]. CPG2-sec included an N-terminal CD8 signal peptide to route the enzyme through the secretory system, and a C-terminal CD8 tail that was found empirically to improve secretion. CPG2-tm also included the CD8 transmembrane domain to anchor the enzyme to the membrane. Both enzymes were expressed effectively, with only CPG2-sec detected in the cell supernatant fluid (Supplementary Fig. 5).

We then tested the ability of the HEK293T-expressed CPG2 to activate cytotoxicity of the AMS-Glu (**2**) prodrug against SET2 leukemia cells. Supernatant fluid from cells expressing CPG2-sec, but not control cells expressing eGFP (enhanced green fluorescent protein), activated dose-dependent cytotoxicity of AMS-Glu (**2**) (CellTiter-Glo assay), with potency comparable to that of the parent drug AMS (**1**) (Fig. 2b). As expected, cytotoxicity was not activated by supernatant fluid from cells expressing CPG2-tm (Fig. 2c). AMS-Glu (**7**) also exhibited dose-dependent cytotoxicity in direct treatment of HEK293T cells expressing CPG2-sec or CPG2-tm, but not control cells (Fig. 2d). Taken together, these results indicate that both enzymes were expressed in active form, with CPG2-sec in the cell supernatant fluid while CPG2-tm remained cell-associated. Given the higher effectiveness of the secreted form in these studies, we elected to advance it further below, while membrane-anchored forms remain an option for future implementations.

For the Ceph-AMS (**3**) prodrug, we focused on the secreted form of β-Lac (β-Lac-sec) (Fig. 2e). β-Lac-sec lacking an endogenous signal peptide was found empirically to be secreted in active form when expressed in HEK293T cells (Supplementary Fig. 6). Supernatant fluid from these cells, but not control cells, activated potent, dose-dependent cytotoxicity of the prodrug Ceph-AMS (**3**) (Fig. 2f). The prodrug also exhibited dose-dependent cytotoxicity in direct treatment of HEK293T cells expressing β-Lac-sec, but not control cells (Fig. 2g). This provided a second enzyme–prodrug pair for further investigations.

Engineering of CPG2 and β-Lac SEAKER cells. We next incorporated the enzymes into an established CAR-T cell platform to generate SEAKER cells[33]. The parent CAR cassette (19BBz) includes an anti-CD19 scFv (single-chain variable fragment) domain, a 4-1BB costimulatory domain and a CD3 zeta chain (Fig. 3a). We engineered new constructs with secreted CPG2 or β-Lac positioned upstream of the CAR cassette, separated by a P2A self-cleaving peptide[34].

The CPG2-19BBz and β-Lac-19BBz constructs were first transduced in the Jurkat T cell line for initial characterization. The secreted enzymes were detected in supernatant fluid from the transduced cells (Supplementary Fig. 7a), and the anti-CD19 CAR module remained functional, based on increased expression of the T cell activation marker CD69, observed in coculture experiments with target Raji ($CD19^+$) Burkitt's lymphoma cells, but not control SET2 ($CD19^-$) leukemia cells (Supplementary Fig. 7b).

Next, primary human T cells from healthy donors were transduced with the CPG2-19BBz and β-Lac-19BBz constructs, and expression of the anti-CD19 CAR module was confirmed by flow cytometry (Supplementary Fig. 8a). The activity of the CAR module was confirmed in coculture experiments with Raji target cells, in which antigen-dependent cytotoxicity was observed for both the CPG2-19BBz and β-Lac-19BBz SEAKERs at levels comparable to the parent 19BBz CAR-T cells (Fig. 3b). Further, comparable levels of proinflammatory cytokines were detected in the supernatant fluids from both classes of SEAKER cells and the parent 19BBz CAR-T cells in cocultures with Raji target cells (Supplementary Fig. 8b). Both SEAKER cell classes also exhibited intrinsic in vivo antitumor efficacy comparable to that of the parent 19BBz CAR-T cells in a Raji xenograft model (Fig. 3c).

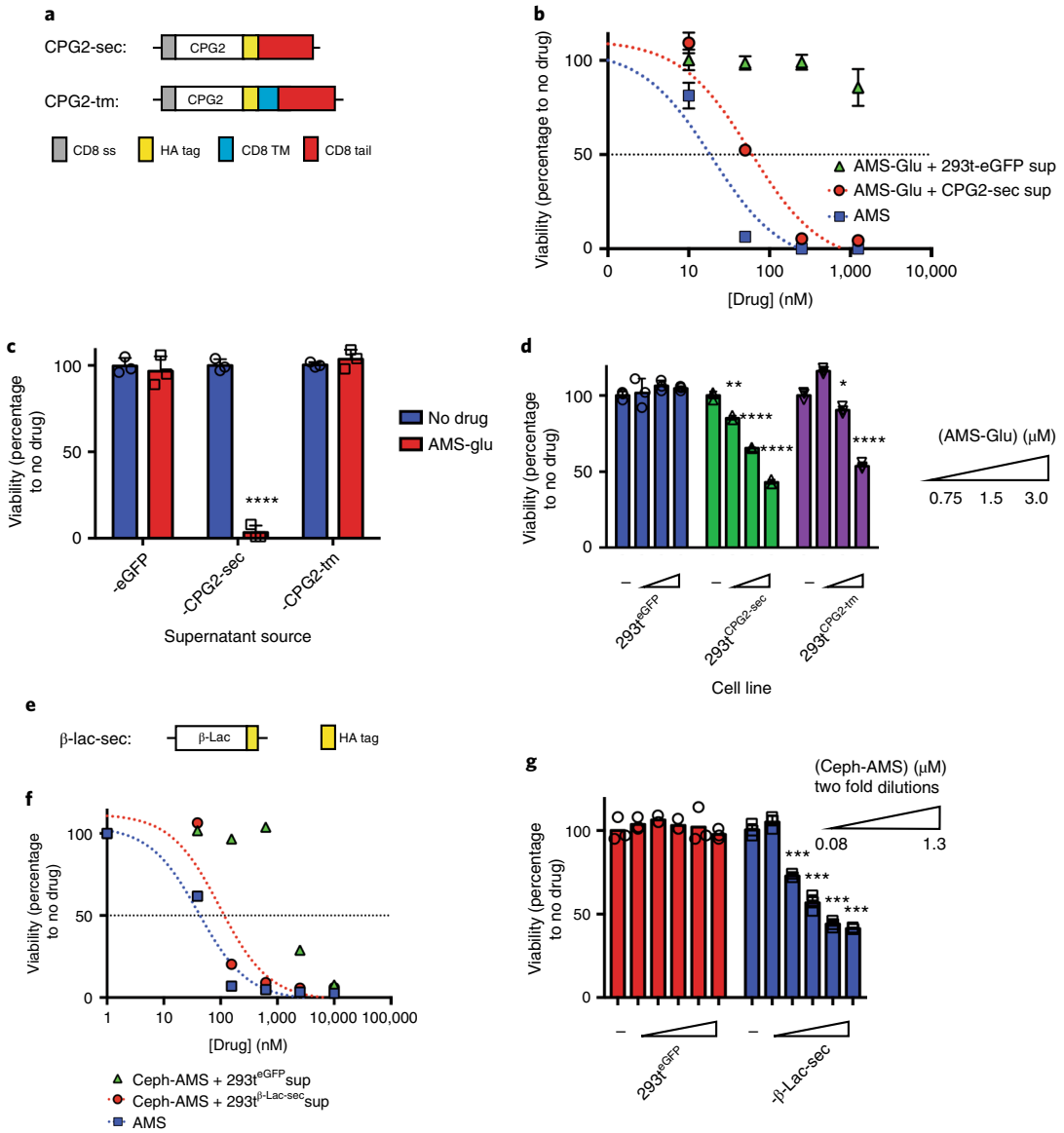

Fig. 2 | In vitro validation of prodrug activation by CPG2- and β-Lac-expressing HEK293T cells. a, CPG2 gene cassettes generated for eukaryotic expression: CPG2-sec (secreted), CPG2-tm (membrane-anchored). CD8 ss, CD8 signal peptide (gray); CPG2, native CPG2 gene excluding endogenous signal peptide (amino acids 1–22) (white); HA tag, hemagglutinin epitope tag (yellow); CD8 TM, CD8 transmembrane domain (blue); CD8 tail, CD8 cytosolic tail (red). **b**, *Trans*-cytotoxicity (against other cell lines) of supernatant fluids from HEK293T-CPG2-sec cells (red circles) or control cells (green triangles) with increasing concentrations of prodrug AMS-Glu (**2**), or of parent drug AMS (**1**) (blue squares), against SET2 target cells (48 h, CellTiter-Glo assay). **c**, *Trans*-cytotoxicity of supernatant fluids from HEK293T-eGFP, -CPG2-sec and -CPG2-tm cell lines, with or without AMS-Glu (**2**, 5 μM) against SET2 target cells (48 h, CellTiter-Glo assay). **d**, *Cis*-cytotoxicity (self-killing) of increasing concentrations of AMS-Glu (**2**) to HEK293T-eGFP, -CPG2-sec and -CPG2-tm cell lines (96 h, CellTiter-Glo assay). **e**, β-Lac-sec (secreted) gene cassette generated for eukaryotic expression: β-Lac, native β-Lac gene excluding endogenous signal peptide (amino acids 1–20) (white) and HA tag, hemagglutinin epitope tag (yellow). **f**, *Trans*-cytotoxicity of supernatant fluids from HEK293T-β-Lac-sec cells (red circles) or control cells (green triangles) with increasing concentration of prodrug Ceph-AMS (**3**), or of parent drug AMS (**1**) (blue squares), against SET2 target cells (48 h, CellTiter-Glo). **g**, *Cis*-cytotoxicity of increasing concentrations of Ceph-AMS (**3**) to HEK293T-eGFP and HEK293T-β-Lac-sec cell lines (48 h, CellTiter-Glo). (For **b**–**d**; **f**–**g**: mean ± s.d. of $n = 3$ biological replicates; Student's two-tailed *t*-test: $^{*}P < 0.05$, $^{**}P < 0.01$, $^{***}P < 0.001$, $^{****}P < 0.0001$; representative of two or more experiments.)

Activation of prodrugs by SEAKER cells. We then tested the ability of the SEAKER-secreted enzymes to activate cytotoxicity of the corresponding prodrugs. CPG2-sec and β-Lac-sec were detected in the supernatant fluids from CPG2-19BBz and β-Lac-19BBz SEAKER cells, respectively (Supplementary Fig. 8c). Coculturing the SEAKERs with Raji target cells, but not SET2 control cells, resulted in significant increases in enzyme concentrations (Fig. 3d). This is consistent with expected antigen-dependent expansion of the SEAKER cells, although general antigen-induced upregulation of enzyme expression is also possible. The activity of CPG2-sec was confirmed using a methotrexate cleavage assay[35] (Supplementary Fig. 8d,e), while β-Lac-sec activity was assessed using a nitrocefin cleavage assay[36] (Supplementary Fig. 8f). Moreover, the supernatant fluids from the SEAKER cells activated the cytotoxicity of the corresponding prodrugs against SET2 cells (Fig. 3e). Taken together, these data showed that both classes of SEAKER cells maintained their intrinsic CAR-T cell functions while also gaining the capability to activate corresponding small-molecule prodrugs.

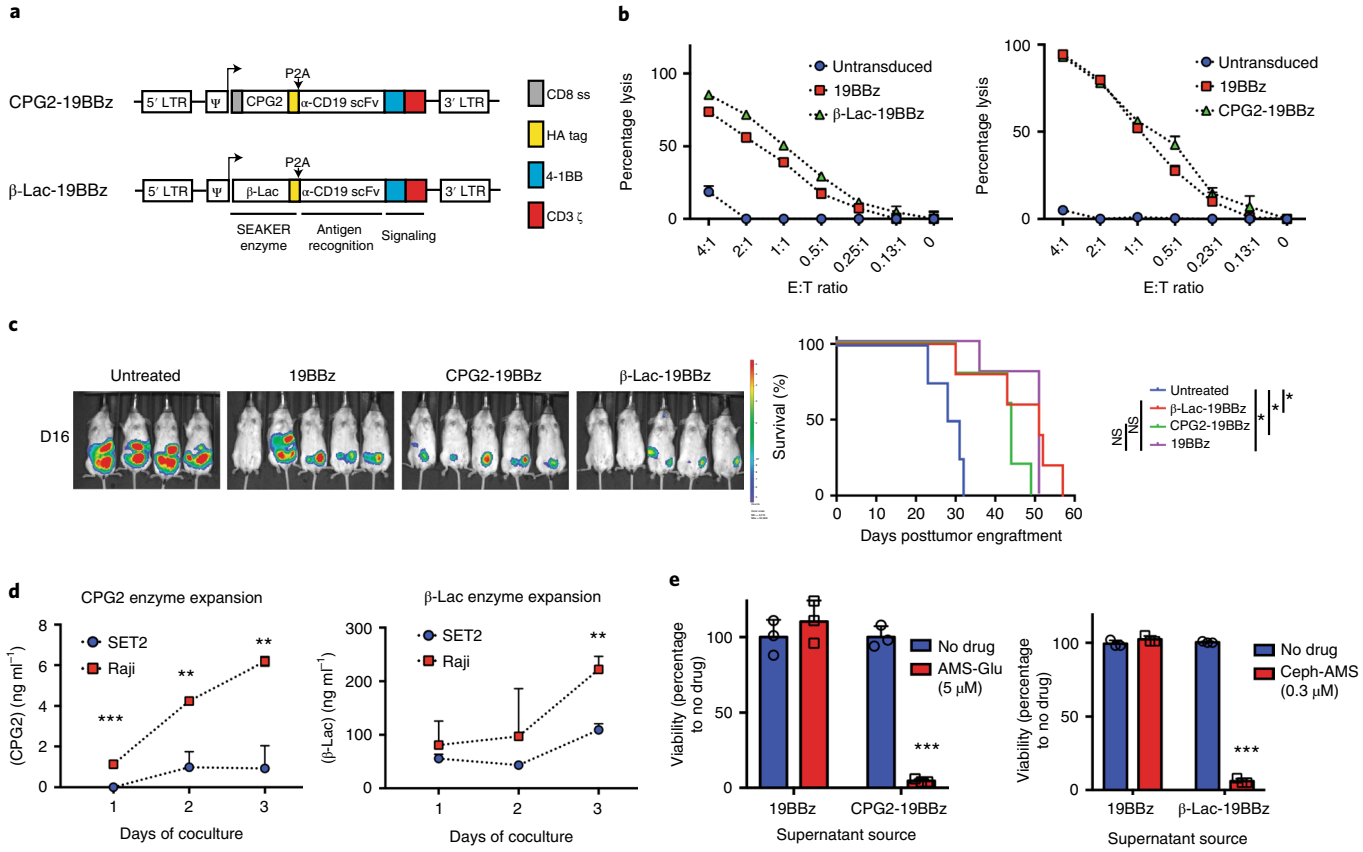

Fig. 3 | Construction and characterization of CPG2- and β-Lac-expressing SEAKER cells. a, SEAKER CAR constructs encoding secreted prodrug-activating enzymes: CPG2-19BBz (CPG2/α-CD19/4-1BB/CD3ζ) and β-Lac-19BBz (β-Lac/α-CD19/4-1BB/CD3ζ). LTR, long terminal repeat; Ψ, psi packaging element; CD8 ss, CD8 signal peptide (gray); HA tag, hemagglutinin epitope tag (yellow); P2A; 2A self-cleaving peptide; α-CD19 scFv, CD19-specific single-chain variable fragment; 4-1BB, 4-1BB costimulatory domain (blue); CD3ζ, CD3 zeta chain (red). **b**, Cytolytic activity of standard 19BBz CAR-T cells, CPG2-19BBz SEAKER cells and β-Lac-19BBz SEAKER cells against Raji (CD19⁺) target cells expressing firefly luciferase (18 h, bioluminescence assay; mean ± s.d. of $n = 3$ biological replicates; representative data from three independent donors). **c**, Antitumor efficacy of standard 19BBz CAR-T cells, CPG2-19BBz SEAKER cells and β-Lac-19BBz SEAKER cells, without prodrugs, against Raji xenografts in NSG mice (day 16 posttumor engraftment, bioluminescent imaging (left) and Kaplan–Meier curve (right). (log-rank (Mantel–Cox) test: $^*P < 0.05$; untreated versus β-Lac-19BBz: $P = 0.003$; untreated versus CPG2-19BBz: $P = 0.023$; Untreated versus 19BBz: $P = 0.03$. Experiment was performed once.) **d**, SEAKER enzyme expression in cocultures of anti-CD19 SEAKER cells with Raji (CD19⁺) or SET2 (CD19⁻) cells (CPG2, ELISA; β-Lac, nitrocefin cleavage ultraviolet assay; mean ± s.d. of $n = 3$ biological replicates; Student's two-tailed t-test: $^{**}P < 0.01$, $^{***}P < 0.001$; representative of three experiments). **e**, *Trans*-cytotoxicity of supernatant fluids from standard 19BBz CAR-T cells and SEAKER cells, with or without the corresponding prodrug, against SET2 target cells (48 h, CellTiter-Glo) (mean ± s.d. of $n = 3$ biological replicates; Student's two-tailed t-test: $^{**}P < 0.01$, $^{***}P < 0.001$).

Enhanced activity of SEAKER–prodrug combinations in vitro. To test whether the SEAKER cells would exhibit enhanced antitumor activity in vitro when combined with the corresponding prodrugs, we carried out coculture experiments of CPG2-19BBz or β-Lac-19BBz SEAKER cells with Raji target cells. Addition of the corresponding AMS-Glu (**2**) or Ceph-AMS (**3**) prodrug, respectively, resulted in significantly enhanced cytotoxicity, which was especially pronounced at low effector-to-target (E:T) ratios (Fig. 4a,b). In contrast, no increase in cytotoxicity was observed when the prodrugs were combined with standard 19BBz CAR-T cells (Fig. 4c,d). Enhanced anticancer activity with Ceph-AMS (**3**) was also observed for the β-Lac-19BBz SEAKER cells against a SKOV-3 ovarian carcinoma solid tumor cell line engineered to express CD19 (Supplementary Fig. 9).

Activity against antigen-negative cancer cells in vitro. We next investigated whether the SEAKER–prodrug combinations could also kill antigen-negative cancer cells in vitro in coculture experiments with both Raji target and SET2 control cells. In the case of the CPG2-19BBz SEAKER cells, treatment with the SEAKER cells alone eliminated the antigen-positive Raji cells, but not the antigen-negative SET2 cells (Fig. 4e,f). In contrast, addition of the AMS-Glu (**2**) prodrug resulted in elimination of both the Raji and SET2 cells, showing antigen-agnostic killing by the activated parent drug AMS (**1**). Notably, under these experimental conditions, the SEAKER cells survived, which may be due to the roughly 1-log lower sensitivity to AMS (**1**) observed for 19BBz CAR-T cells compared to the Raji and SET2 cells (Supplementary Table 1). Similar results were also observed for the β-Lac-19BBz SEAKER cells with and without the corresponding Ceph-AMS (**3**) prodrug (Fig. 4g).

Enhanced efficacy of SEAKER–prodrug combinations in vivo. Toward evaluating the antitumor efficacy of the SEAKER systems in mouse models, we analyzed the in vitro pharmacological properties and in vivo pharmacokinetics of AMS-Glu (**2**) and Ceph-AMS (**3**). Both prodrugs were stable in mouse and human plasma and liver microsomes, and exhibited acceptable plasma protein binding (Supplementary Table 3). In single-dose pharmacokinetic

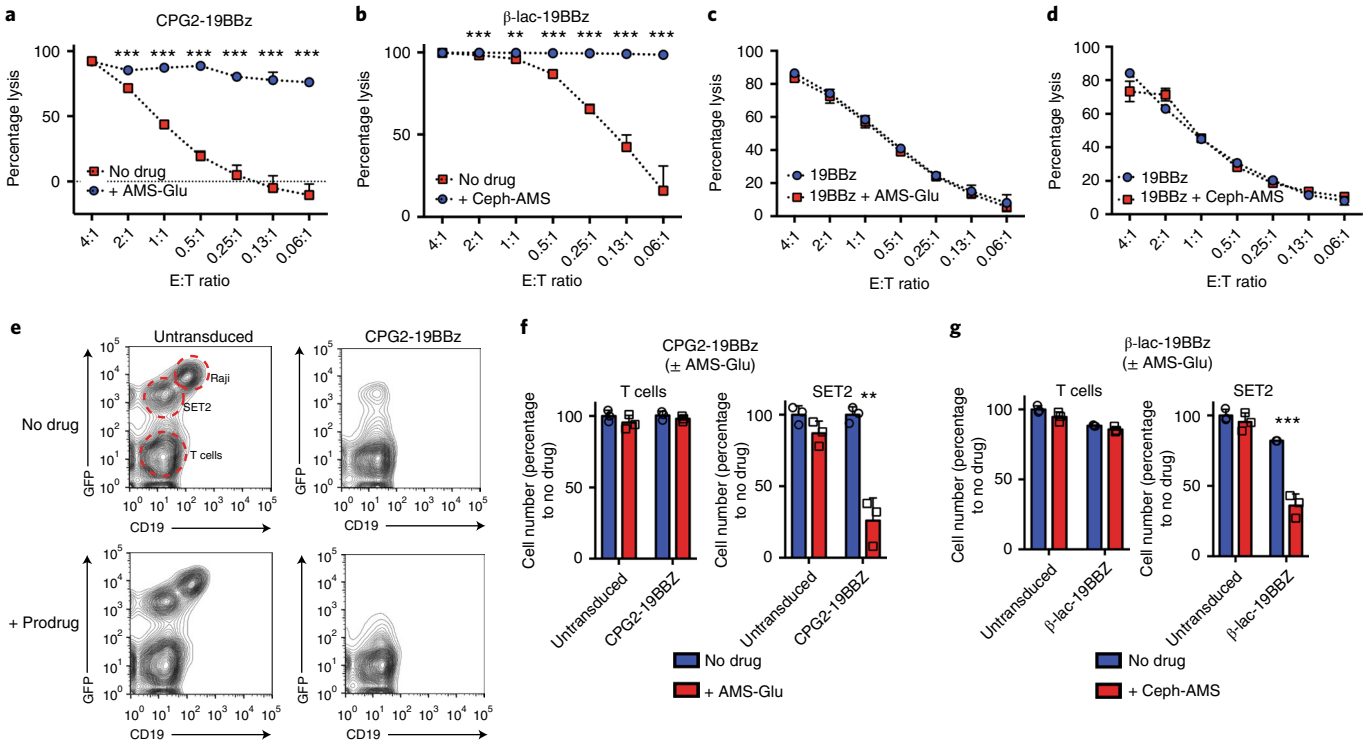

Fig. 4 | In vitro validation of prodrug activation by SEAKER cells and antigen-negative cell killing. a, Specific lysis by CPG2-19BBz SEAKER cells, with and without AMS-Glu (**2**, 20 μM), against Raji (CD19⁺) target cells expressing firefly luciferase (18–96 h, bioluminescence assay). **b**, Specific lysis of β-Lac-19BBz SEAKER cells, with and without Ceph-AMS (**3**, 0.3 μM), as in **a**. **c**,**d**, Specific lysis by 19BBz CAR-T cells, with and without AMS-Glu (**2**) (**c**) or Ceph-AMS (**3**) (**d**) against Raji (CD19⁺) target cells expressing firefly luciferase (48 h, bioluminescence assay). **e**, Flow cytometric analysis of *trans*-cytotoxicity of CPG2-19BBz SEAKER cells, with and without AMS-Glu (**2**, 20 μM), against Raji (CD19⁺) antigen-positive cells and SET2 (CD19⁻) antigen-negative cells engineered to express eGFP (representative data from two donors). **f**, Quantitation of cell numbers from coculture experiments in **e**. **g**, Quantitation of cell numbers from flow cytometric analysis of *trans*-cytotoxicity of β-Lac-19BBz SEAKER cells, with and without Ceph-AMS (**3**, 0.3 μM), against Raji (CD19⁺) antigen-positive cells and SET2 (CD19⁻) antigen-negative cells. (For **a**–**g**, mean ± s.d. of $n = 3$ biological replicates; Student's two-tailed *t*-test: $^{**}P < 0.01$, $^{***}P < 0.001$; representative data from three or more independent donors.)

experiments in mice, both prodrugs provided plasma C_{max} (maximum concentration) values well above the in vitro IC_{50} values at modest doses (10 and 5 mg kg^{-1}, intraperitoneal (i.p.), respectively), albeit with short plasma half-lives ($t_{1/2} < 1$ h). Notably, AMS (**1**) (0.5 mg kg^{-1}, i.p.) also exhibited a very short plasma half-life in vivo ($t_{1/2} < 0.2$ h). Pilot toxicology studies identified a maximum tolerated dose for AMS-Glu (**2**) of 50 mg kg^{-1} (i.p., b.i.d. (twice a day) × 3 days). For Ceph-AMS (**3**), gross toxicity was observed at 50 mg kg^{-1} after the first day of dosing (i.p., b.i.d.), so a lower 4 mg kg^{-1} dose was selected for use in efficacy studies below.

We also investigated the pharmacokinetics of CAR-T cells in mice to determine the optimal time for prodrug administration. We engineered 19BBz CAR-T cells to express a membrane-anchored form of *Gaussia* luciferase (gLuc-19BBz), which could be imaged in vivo by administration of a coelenterazine substrate[37] (Supplementary Fig. 10a). These cells exhibited in vitro cytotoxicity comparable to that of standard 19BBz CAR-T cells against Raji target cells engineered to express eGFP and firefly luciferase (Raji-eGFP/fLuc) (Supplementary Fig. 10b). NSG (NOD-SCID-gamma) mice engrafted i.p. with Raji-eGFP/fLuc (CD19⁺) tumors were treated i.p. 2 days later with gLuc-19BBz CAR-T cells. Bioluminescent imaging revealed that CAR-T cell levels increased rapidly by roughly 2 logs in the first day, then remained relatively steady for at least 33 days (Supplementary Fig. 10c), indicating that prodrug treatment could begin any time after the first day following CAR-T cell administration.

To assess whether the SEAKER cells could produce active enzymes in vivo, NSG mice were engrafted i.p. with Raji-eGFP/fLuc (CD19⁺) tumors, then treated 2 days later i.p. with CPG2-19BBz or β-Lac-19BBz SEAKER cells. Two days after SEAKER administration, samples from peritoneal lavage (ascites) and peripheral blood were assessed for enzyme activity. In both cases, the active enzymes were detected and were restricted to the peritoneum and not detected in peripheral blood (Fig. 5a,b).

Finally, to determine whether the SEAKER cells could activate the antitumor activity of the prodrugs in vivo, mice engrafted i.p. with Raji-eGFP/fLuc (CD19⁺) tumors were treated 2 days later i.p. with CPG2-19BBz or β-Lac-19BBz SEAKER cells, at dose levels lower than necessary for full tumor clearance by immune cell cytolysis alone, followed 2 days after SEAKER administration by the corresponding prodrug AMS-Glu (**2**) or Ceph-AMS (**3**), respectively (Fig. 5c). Decreased tumor bioluminescence was observed in mice treated with both the SEAKER cells and corresponding prodrug, compared to SEAKER cells alone (Fig. 5d,e and Extended Data Fig. 3). This effect was not observed in mice treated with standard 19BBz CAR-T cells plus either prodrug, consistent with specific activation of the prodrugs by only the SEAKER cells. The parent drug AMS (**1**) could not be used as a control because it is highly toxic (single-dose LD_{50} <0.4 mg kg^{-1}, i.p., Ha/ICR mice[26]), and systemic administration at these 10–100-fold higher dose levels would be lethal and unethical. We did not observe overt systemic toxicity in these experiments.

Efficacy against antigen-negative cancer cells in vivo. To test whether the SEAKER–prodrug combination would have efficacy against antigen-negative cells in the context of a heterogeneous tumor in vivo, much like that encountered in a human patient with

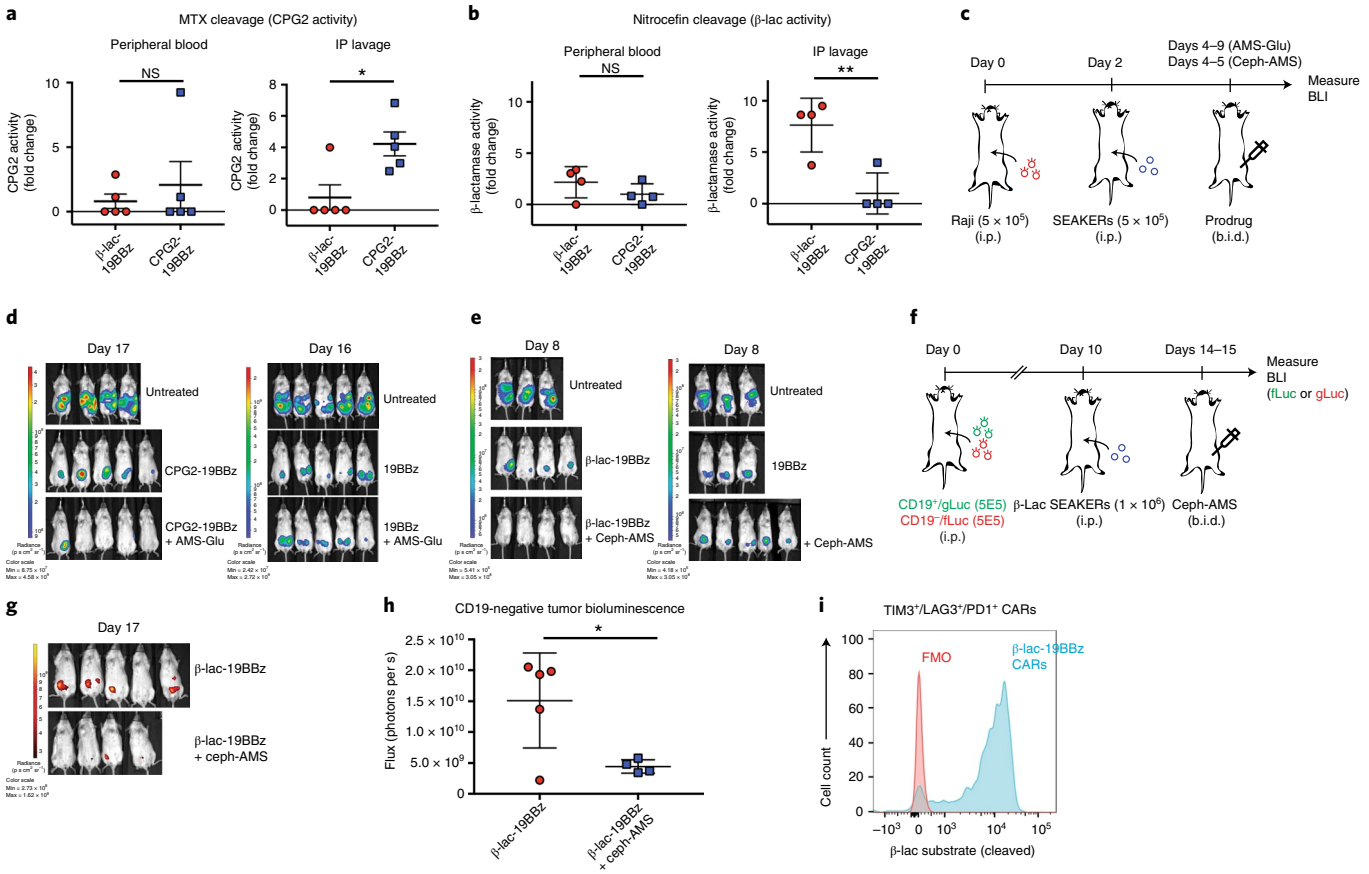

Fig. 5 | Enhanced in vivo efficacy of prodrug–SEAKER cell combinations in mouse i.p. xenografts. a, CPG2 enzyme activity in peripheral blood (left) or peritoneal lavage (right) of Raji tumor-engrafted NSG mice treated with CPG2-19BBz SEAKER cells or β-Lac-19BBz SEAKER cells (negative control), based on methotrexate cleavage assay (fold-change; mean ± s.d. of $n = 5$ mice per group; Student's two-tailed t-test: $^*P < 0.05$; representative data from two independent experiments). **b**, β-Lac enzyme activity in peripheral blood (left) or peritoneal lavage (right) of Raji tumor-engrafted mice treated with CPG2-19BBz SEAKER cells (negative control) or β-Lac-19BBz SEAKER cells, based on nitrocefin cleavage assay (fold-change; mean ± s.d. of $n = 4$ mice per group; Student's two-tailed t-test: $^{**}P < 0.01$; representative data from two independent experiments). **c**, Experimental scheme to assess efficacy of SEAKER–prodrug combinations in i.p. tumor model (AMS-Glu (**2**): 50 mg kg^{-1}, i.p., b.i.d., 12 doses in total; Ceph-AMS (**3**): 4 mg kg^{-1}, i.p., b.i.d., three doses in total). **d**,**e**, Tumor bioluminescence was monitored over time in mice treated with CPG2-19BBz (**d**) or β-Lac-19BBz (**e**) SEAKER cells, or with 19BBz CAR T cells (control), with or without the corresponding prodrug (representative images shown; experiment in **e** was repeated with similar results) (see also Extended Data Fig. 3). **f**, Experimental scheme to assess efficacy in a heterogeneous tumor model (2×10^6 total cells, 1:1 Nalm6-mCherry/gLuc (CD19$^+$) and Nalm6-eGFP/fLuc (CD19$^-$) (Ceph-AMS (**3**): 4 mg kg^{-1}, i.p., b.i.d., three doses total). **g**,**h**, Antitumor efficacy against CD19$^-$ Nalm6 cancer cells (fLuc) engrafted within the heterogeneous tumor with CD19$^+$ Nalm6 cancer cells (Extended Data Fig. 4), only in mice receiving β-Lac-19BBz SEAKER cells plus Ceph-AMS prodrug (**3**) (representative images shown on day 17 from a 20-day study (**g**); one mouse in prodrug-treated group died between days 14 and 17 and is omitted) (tumor bioluminescence on day 17 (**h**): mean ± s.d. of $n = 5$ mice in SEAKER-treated group and $n = 4$ mice in SEAKER + prodrug-treated group; Student's two-tailed t-test: $^*P < 0.05$; experiment was performed once). **i**, Retention of β-Lac enzyme activity in β-Lac-19BBz SEAKER cells expressing T cell exhaustion markers (TIM3, LAG3, PD1) after 26 days in Raji-engrafted mice (flow cytometry analysis: FMO, fluorescence minus one control; β-Lac substrate, CCF2-AM) (representative data shown for one of $n = 4$ mice; representative data from two independent experiments).

cancer, we used a mixed tumor model composed of Nalm6 (CD19$^+$) leukemia cells engineered to express mCherry and *Gaussia* luciferase (Nalm6-mCherry/gLuc (CD19$^+$)) and Nalm6 cells with the CD19 antigen knocked out by CRISPR–Cas9 deletion and engineered to express eGFP and firefly luciferase (Nalm6-eGFP/fLuc (CD19$^-$)). NSG mice were engrafted with a 1:1 mixture of these cells, treated 10 days later i.p. with β-Lac-19BBz SEAKER cells, then treated 2 days later with the Ceph-AMS (**3**) prodrug (Fig. 5f). Significant killing of the antigen-negative cells was observed in mice treated with both the SEAKER cells and prodrug, but not the SEAKER cells alone (Fig. 5g,h and Extended Data Fig. 4a,b). Again, overt systemic toxicity was not observed in these experiments.

SEAKER enzyme activity persistence after T cell exhaustion. One cause of potential failure of CAR-T cells is exhaustion of their immune cytotoxic functions over time due to chronic antigen stimulation. We examined whether SEAKER cells that have become exhausted would maintain expression and activity of a prodrug-activating enzyme. NSG mice were engrafted i.p. with Raji-eGFP/fLuc tumors, then treated 2 days later i.p. with β-Lac-19BBz SEAKER cells. SEAKER cells extracted from the mice 26 days later displayed the exhaustion markers TIM3, LAG3 and PD1, but >90% of those cells continued to exhibit β-Lac enzyme activity (Fig. 5i and Supplementary Fig. 11). Moreover, in mice that had also been treated with Ceph-AMS (**3**) on days 4–5 posttumor engraftment, administration of a second round of prodrug beginning on day 22 led to a >1-log decrease in tumor burden (Extended Data Fig. 5a,b). SEAKER cells extracted from these mice by peritoneal lavage on day 30 posttumor engraftment continued to exhibit β-Lac enzyme activity, indicating their survival and continued prodrug-activating

capability even after two courses of prodrug treatment (Extended Data Fig. 5c).

SEAKER–prodrug efficacy in subcutaneous tumor models. We next investigated whether the SEAKER–prodrug combinations would be efficacious in a subcutaneous tumor model. NSG mice were engrafted subcutaneously (s.c.) with Raji-eGFP/fLuc (CD19$^+$) tumor cells and pharmacokinetic studies were again carried out using gLuc-19BBz CAR-T cells[37], injected intravenously (i.v.) 7 days after tumor engraftment. Bioluminescent imaging indicated that the CAR-T cells expressing membrane-anchored *Gaussia* luciferase aggregated at the tumor with peak concentrations at 9 days after administration (Supplementary Fig. 12).

In a key demonstration of the SEAKER concept, we showed that SEAKER cells produced active enzyme in vivo at the tumor site. NSG mice were engrafted s.c. with Raji-eGFP/fLuc (CD19$^+$) tumors as above, then treated 7 days later i.v. with β-Lac-19BBz SEAKER cells. Tumors were resected 9 days after SEAKER administration and β-Lac enzyme activity was detected in the tumor (Fig. 6a). By contrast, β-Lac enzyme activity was not detected in the spleen, a natural clearing site of CAR-T cells, consistent with localized distribution in the tumor (Supplementary Fig. 13). Moreover, immunohistochemistry staining of the resected tumors using an anti-β-Lac antibody revealed loci of concentrated staining, with additional diffuse staining throughout the tumor, consistent with diffusion of the enzyme away from the SEAKER cells and throughout the tumor (Fig. 6b).

We then evaluated whether the SEAKER–prodrug combinations exhibited enhanced antitumor efficacy in this model. NSG mice were engrafted s.c. with Raji-eGFP/fLuc (CD19$^+$) tumors, then treated 7 days later i.v. with CPG2 or β-Lac SEAKER cells as above (Fig. 6c). Beginning 8 days after SEAKER administration, the mice were treated with the corresponding prodrug, AMS-Glu (**2**) or Ceph-AMS (**3**), respectively. Mice treated with both the SEAKER cells and corresponding prodrug showed significantly extended survival compared to those treated with the SEAKER cells alone and untreated control mice (Fig. 6d). We did not observe overt systemic toxicity in these experiments (Supplementary Fig. 14). Attempts to quantitate the concentration of the activated drug AMS (**1**) in tumors were complicated by the high variability at any single timepoint, which is influenced by differences in tumor size, SEAKER cell localization, prodrug concentration, enzymatic activation of the prodrug and clearance of the activated drug, in contrast to antitumor efficacy, which reflects integration of drug concentration across the entire experiment. Notably, the prodrugs did not significantly extend survival of mice treated with standard 19BBz CAR-T cells (Supplementary Fig. 15), again consistent with specific activation of the prodrugs by only the SEAKER cells.

Immunogenicity of SEAKER cells in a syngeneic mouse model. To investigate whether an intact immune system would neutralize the bacterial enzymes expressed by the SEAKER cells, we used a syngeneic mouse tumor model[16]. We constructed murine SEAKER cells expressing β-Lac and a CAR comprising an anti-MUC16 scFv domain, a mouse CD28 costimulatory domain and a mouse CD3 zeta chain (β-Lac-MUC28z), from primary murine T cells (Extended Data Fig. 6a,b). The anti-MUC16 CAR was used instead of the anti-CD19 CAR used above to avoid depletion of healthy B cells that would confound a potential antibody response to the bacterial enzyme. We confirmed that supernatant fluid from these cells activated the cytotoxicity of Ceph-AMS (**3**) against mouse EL4 lymphoma tumor cells in vitro (Extended Data Fig. 6c). Next, immunocompetent C57BL/6 mice were engrafted i.p. with murine ID8 ovarian surface epithelial cells that express MUC16, then treated 21 days later i.p. with β-Lac-MUC28z SEAKER cells (Extended Data Fig. 7a). Mice were preconditioned with cyclophosphamide before SEAKER cell administration to facilitate engraftment, a regimen that is also used in the clinic. Sera collected from mice over 10 days were analyzed for IgG reactivity to recombinant β-Lac, revealing the development of anti-β-Lac antibodies in most of the mice (Extended Data Fig. 7b). Analysis of ascites showed that the murine SEAKER cells persisted in mice at least 7 days after administration (Extended Data Fig. 7c,d). Moreover, these samples retained full β-Lac enzyme activity (Extended Data Fig. 7e). We further demonstrated that anti-β-Lac-containing sera from SEAKER-treated mice (without preconditioning to provide a maximal immune response) did not inhibit the enzymatic activity of recombinant β-Lac in vitro (Extended Data Fig. 7f,g). Taken together, these results show that, in this syngeneic model, although SEAKER cells are immunogenic as expected, the resulting immune response does not result in early clearance of the SEAKER cells nor in neutralization of β-Lac enzymatic activity ex vivo.

Discussion

The SEAKER cell platform established herein provides a potential means to overcome some of the current limitations of CAR-T cells[5], through targeted, local activation of small-molecule drugs with orthogonal activity. We have shown that SEAKER–prodrug combinations provide enhanced anticancer activity in vitro and in vivo, with the important added function of killing of antigen-negative cells in heterogeneous tumors. The SEAKER cells maintain prodrug-activating activity even after becoming immunologically exhausted. The secreted enzymes and activated drugs can diffuse throughout tumors, of potential benefit in solid tumors. Further, SEAKERs provide multiple layers of local drug amplification via cell proliferation, enzyme production and catalytic prodrug activation, in contrast to other drug delivery systems such as antibody–drug conjugates and ADEPT.

We demonstrated this modularity of the SEAKER platform using three classes of small-molecule drugs with different mechanisms of action. Of course, a wide range of other drugs can be envisioned depending on intended therapeutic applications, including those outside cancer, and many such drugs have been explored previously in the context of ADEPT[22]. Differences in enzyme kinetics and the relative sensitivity of the SEAKER cells and target cells to the activated drug will be important considerations in future applications. Other enzyme transformations can be also envisioned to avoid the use of large masking groups that dominate pharmacological properties.

We envisioned that secreted enzymes would provide higher levels of prodrug activation, while membrane-anchored forms could provide more tightly localized prodrug activation and potentially reduce off-tumor toxicity. In the mouse xenograft models herein, we did not observe appreciable off-tumor toxicity with the secreted enzymes. However, membrane-anchored variants may still be of interest if systemic toxicity proves limiting.

Potential immunogenicity of bacterial enzymes is an important consideration for future translation, as neutralizing antibodies may block their activity[38]. This may be addressed by using deimmunized forms of the enzymes[31] that were developed subsequently to the initial ADEPT clinical trials[39], through coadministration of immunosuppressants that do not interfere with T cell functions[40,41] or by using human enzymes[42–44]. Notably, it is well established that CAR-T cells are, themselves immunogenic[45], but this has not impeded their effective use in the clinic, as they act through a rapid period of tumor lysis that occurs before the humoral immune response is fully mounted. Further, many nonhuman enzymes are Food and Drug Administration approved, widely prescribed and used safely[38].

We used herein a well-established anti-CD19 CAR-T cell system that has been clinically validated[46], but SEAKER cells can readily be targeted to other antigens to treat a variety of cancers, including solid tumors in which the diffusible small-molecule drug could be particularly valuable, as well as potentially other diseases requiring local delivery of a small-molecule drug that would otherwise cause dose-limiting toxicity if administered systemically.

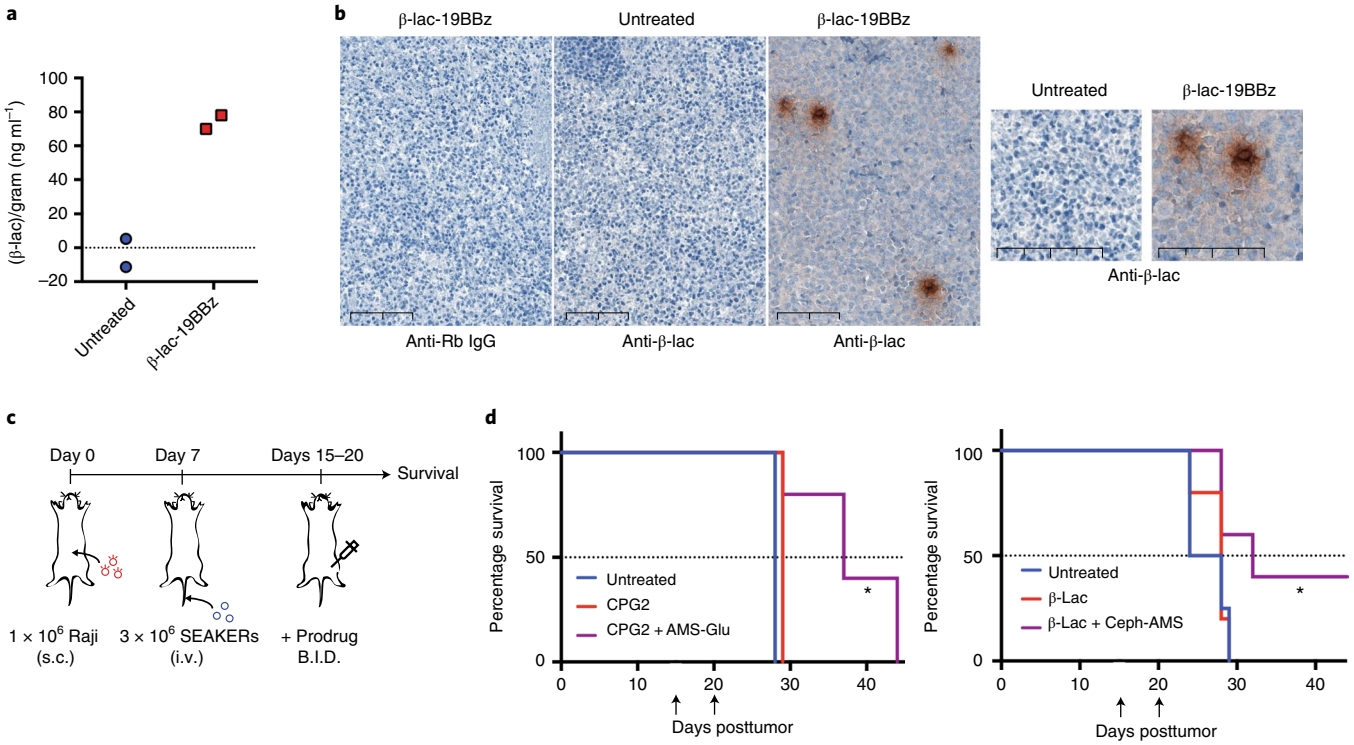

Fig. 6 | Enhanced in vivo efficacy of Ceph-AMS–β-Lac SEAKER cell combinations in mouse subcutaneous xenografts. a, Nitrocefin cleavage-based quantitation of tumor β-Lac concentration in a subcutaneous Raji tumor from a mouse treated with 3×10^6 β-Lac-19BBz SEAKER cells (i.v., intravenous) (representative data from two of $n=5$ mice per group in three independent experiments). **b**, Anti-β-Lac immunohistochemistry imaging of subcutaneous Raji tumors extracted on day 15 from mice that were untreated, or received 3×10^6 β-Lac-19BBz SEAKER cells (i.v.) (top panels: left, isotype control; center, untreated mouse stained with anti-β-Lac antibody; right, β-Lac-19BBz-treated mouse stained with anti-β-Lac antibody). Increased magnification highlights diffuse β-Lac staining throughout the tumor environment (right panels) (representative data shown from one of the three remaining mice from the $n=5$ group used in **a**). Scale bars, 100 µm. **c**, Experimental scheme to assess therapeutic efficacy of SEAKER–prodrug combinations in a subcutaneous (s.c.) solid tumor model. Raji tumor cells were engrafted s.c. on day 0 followed by SEAKER cells i.v. on day 7. The corresponding prodrug was administered beginning on day 15 (AMS-Glu (**2**): 50 mg kg^{-1}, i.p., b.i.d., days 15–20, total of 12 doses or Ceph-AMS (**3**): 4 mg kg^{-1}, i.p., b.i.d. every other day, days 15, 17 and 19, total of 6 doses) and mice were monitored for survival. **d**, Survival analysis of mice engrafted with subcutaneous Raji tumors receiving subtherapeutic doses of CPG2-19BBz SEAKER cells (CPG2) plus AMS-Glu (**2**) (left panel) or β-Lac-19BBz SEAKER cells (β-Lac) plus Ceph-AMS (**3**) (right panel). (Arrows denote the beginning and end of the prodrug administration period; $n=5$ mice per group; log-rank (Mantel–Cox) test: $^*P<0.05$; CPG2-19BBz versus CPG2-19BBz + AMS-Glu: $P=0.023$; β-Lac-19BBz versus β-Lac-19BBz + Ceph-AMS: $P=0.048$; experiment was repeated with similar results).

This general approach may also be extended to other cell-based therapeutic platforms, such as tumor-infiltrating lymphocytes and synthetic T cell receptor therapy[47–49]. The SEAKER platform remains antigen-dependent and, thus, like other such cellular therapies, may result in off-tumor toxicity based on the antigen selected and would not be effective against completely antigen-negative tumors. However, antigen-negative cell relapse from heterogeneous tumors is a major source of treatment failure with current CAR-T cell therapies, so SEAKER–prodrug combinations could reduce this relapse mechanism.

In conclusion, we have established a new cellular therapeutic platform of targeted 'micropharmacies' that integrates CAR-T cell immunotherapy with local activation of small-molecule prodrugs, exhibits enhanced antitumor activity in vitro and in vivo, and can overcome a variety of current obstacles in conventional CAR-T cell therapy. The platform provides a broadly applicable means to augment cellular therapeutics that may extend to other diseases.

Online content

Any methods, additional references, Nature Research reporting summaries, source data, extended data, supplementary information, acknowledgements, peer review information; details of author contributions and competing interests; and statements of data and code availability are available at https://doi.org/10.1038/s41589-021-00932-1.

Received: 23 December 2020; Accepted: 21 October 2021;
Published online: 30 December 2021

References

1. Feldman, S. A., Assadipour, Y., Kriley, I., Goff, S. L. & Rosenberg, S. A. Adoptive cell therapy—tumor-infiltrating lymphocytes, T-cell receptors, and chimeric antigen receptors. *Semin. Oncol.* **42**, 626–639 (2015).
2. Leon, E., Ranganathan, R. & Savoldo, B. Adoptive T cell therapy: boosting the immune system to fight cancer. *Semin. Immunol.* **49**, 101437 (2020).
3. Sadelain, M., Rivière, I. & Riddell, S. Therapeutic T cell engineering. *Nature* **545**, 423–431 (2017).
4. Beyar-Katz, O. & Gill, S. Advances in chimeric antigen receptor T cells. *Curr. Opin. Hematol.* **27**, 368–377 (2020).
5. June, C. H., O'Connor, R. S., Kawalekar, O. U., Ghassemi, S. & Milone, M. C. CAR T cell immunotherapy for human cancer. *Science* **359**, 1361–1365 (2018).
6. Sermer, D. & Brentjens, R. CAR T-cell therapy: full speed ahead. *Hematol. Oncol.* **37**, 95–100 (2019).
7. Sotillo, E. et al. Convergence of acquired mutations and alternative splicing of CD19 enables resistance to CART-19 immunotherapy. *Cancer Discov.* **5**, 1282–1295 (2015).
8. Maude, S. L. et al. Chimeric antigen receptor T cells for sustained remissions in leukemia. *N. Engl. J. Med.* **371**, 1507–1517 (2014).

9. Majzner, R. G. & Mackall, C. L. Tumor antigen escape from CAR T-cell therapy. *Cancer Discov.* **8**, 1219–1226 (2018).
10. Anderson, K. G., Stromnes, I. M. & Greenberg, P. D. Obstacles posed by the tumor microenvironment to T cell activity: a case for synergistic therapies. *Cancer Cell* **31**, 311–325 (2017).
11. Kasakovski, D., Xu, L. & Li, Y. T cell senescence and CAR-T cell exhaustion in hematological malignancies. *J. Hematol. Oncol.* **11**, 91 (2018).
12. Neelapu, S. S. et al. Chimeric antigen receptor T-cell therapy: assessment and management of toxicities. *Nat. Rev. Clin. Oncol.* **15**, 47–62 (2018).
13. Dunbar, C. E. et al. Gene therapy comes of age. *Science* **359**, eaan4672 (2018).
14. Lim, W. A. & June, C. H. The principles of engineering immune cells to treat cancer. *Cell* **168**, 724–740 (2017).
15. Rafiq, S. et al. Targeted delivery of a PD-1-blocking scFv by CAR-T cells enhances anti-tumor efficacy in vivo. *Nat. Biotechnol.* **36**, 847–856 (2018).
16. Yeku, O. O., Purdon, T. J., Koneru, M., Spriggs, D. & Brentjens, R. J. Armored CAR T cells enhance antitumor efficacy and overcome the tumor microenvironment. *Sci. Rep.* **7**, 10541 (2017).
17. Avanzi, M. P. et al. Engineered tumor-targeted T cells mediate enhanced anti-tumor efficacy both directly and through activation of the endogenous immune system. *Cell Rep.* **23**, 2130–2141 (2018).
18. Boice, M. et al. Loss of the HVEM tumor suppressor in lymphoma and restoration by modified CAR-T cells. *Cell* **167**, 405–418 (2016).
19. Kuhn, N. F. et al. CD40 ligand-modified chimeric antigen receptor T cells enhance antitumor function by eliciting an endogenous antitumor response. *Cancer Cell* **35**, 473–488 (2019).
20. Brudno, J. N. & Kochenderfer, J. N. Recent advances in CAR T-cell toxicity: mechanisms, manifestations and management. *Blood Rev.* **34**, 45–55 (2019).
21. Lambert, J. M. & Berkenblit, A. Antibody-drug conjugates for cancer treatment. *Annu. Rev. Med.* **69**, 191–207 (2018).
22. Sharma, S. K. & Bagshawe, K. D. Translating antibody directed enzyme prodrug therapy (ADEPT) and prospects for combination. *Expert Opin. Biol. Ther.* **17**, 1–13 (2017).
23. Nemunaitis, J. et al. Pilot trial of genetically modified, attenuated *Salmonella* expressing the *E. coli* cytosine deaminase gene in refractory cancer patients. *Cancer Gene Ther.* **10**, 737–744 (2003).
24. Sherwood, R. F., Melton, R. G., Alwan, S. M. & Hughes, P. Purification and properties of carboxypeptidase G2 from *Pseudomonas* sp. strain RS-16. Use of a novel triazine dye affinity method. *Eur. J. Biochem.* **148**, 447–453 (1985).
25. Fleming, P. C., Goldner, M. & Glass, D. G. Observations on the nature, distribution, and significance of cephalosporinase. *Lancet* **1**, 1399–1401 (1963).
26. Jaffe, J. J., McCormack, J. J. & Meymerian, E. Trypanocidal properties of 5′-*O*-sulfamoyladenosine, a close structural analog of nucleocidin. *Exp. Parasitol.* **28**, 535–543 (1970).
27. Rengaraju, S. et al. 5′-*O*-Sulfamoyladenosine (defluoronucleocidin) from a *Streptomyces*. *Meiji Seika Kenkyu Nenpo* **25**, 49–55 (1986).
28. Francis, R. J. et al. A Phase I trial of antibody directed enzyme prodrug therapy (ADEPT) in patients with advanced colorectal carcinoma or other CEA producing tumours. *Br. J. Cancer* **87**, 600–607 (2002).
29. Springer, C. J. et al. Optimization of alkylating agent prodrugs derived from phenol and aniline mustards: a new clinical candidate prodrug (ZD2767) for antibody-directed enzyme prodrug therapy (ADEPT). *J. Med. Chem.* **38**, 5051–5065 (1995).
30. Yoo, B. et al. Ultrasmall dual-modality silica nanoparticle drug conjugates: design, synthesis, and characterization. *Bioorg. Med. Chem.* **23**, 7119–7130 (2015).
31. Harding, F. A. et al. A beta-lactamase with reduced immunogenicity for the targeted delivery of chemotherapeutics using antibody-directed enzyme prodrug therapy. *Mol. Cancer Ther.* **4**, 1791–1800 (2005).
32. Marais, R. et al. A cell surface tethered enzyme improves efficiency in gene-directed enzyme prodrug therapy. *Nat. Biotechnol.* **15**, 1373–1377 (1997).
33. Brentjens, R. J. et al. Genetically targeted T cells eradicate systemic acute lymphoblastic leukemia xenografts. *Clin. Cancer Res.* **13**, 5426–5435 (2007).
34. Liu, Z. et al. Systematic comparison of 2A peptides for cloning multi-genes in a polycistronic vector. *Sci. Rep.* **7**, 2193 (2017).
35. Levy, C. C. & Goldman, P. The enzymatic hydrolysis of methotrexate and folic acid. *J. Biol. Chem.* **242**, 2933–2938 (1967).
36. Bulychev, A. & Mobashery, S. Class C beta-lactamases operate at the diffusion limit for turnover of their preferred cephalosporin substrates. *Antimicrob. Agents Chemother.* **43**, 1743–1746 (1999).
37. Santos, E. B. et al. Sensitive in vivo imaging of T cells using a membrane-bound *Gaussia princeps* luciferase. *Nat. Med.* **15**, 338–344 (2009).
38. Gurung, N., Ray, S., Bose, S. & Rai, V. A broader view: microbial enzymes and their relevance in industries, medicine, and beyond. *BioMed. Res. Int.* **2013**, 329121 (2013).
39. Mayer, A. et al. Modifying an immunogenic epitope on a therapeutic protein: a step towards an improved system for antibody-directed enzyme prodrug therapy (ADEPT). *Br. J. Cancer* **90**, 2402–2410 (2004).
40. Liu, S. et al. Corticosteroids do not influence the efficacy and kinetics of CAR-T cells for B-cell acute lymphoblastic leukemia. *Blood Cancer J.* **10**, 15 (2020).
41. Bagshawe, K. D. & Sharma, S. K. Cyclosporine delays host immune response to antibody enzyme conjugate in ADEPT. in *Proc. International Conference on New Trends in Clinical and Experimental Immunosuppression, Geneva* (1996).
42. Smith, G. K. et al. Toward antibody-directed enzyme prodrug therapy with the T268G mutant of human carboxypeptidase A1 and novel in vivo stable prodrugs of methotrexate. *J. Biol. Chem.* **272**, 15804–15816 (1997).
43. Oosterhoff, D. et al. Secreted and tumour targeted human carboxylesterase for activation of irinotecan. *Br. J. Cancer* **87**, 659–664 (2002).
44. Chen, K. C. et al. Membrane-localized activation of glucuronide prodrugs by beta-glucuronidase enzymes. *Cancer Gene Ther.* **14**, 187–200 (2007).
45. Peraro, L. et al. Incorporation of bacterial immunoevasins to protect cell therapies from host antibody-mediated immune rejection *Mol. Ther.* https://doi.org/10.1016/j.ymthe.2021.06.022 (2021).
46. Porter, D. L., Levine, B. L., Kalos, M., Bagg, A. & June, C. H. Chimeric antigen receptor-modified T cells in chronic lymphoid leukemia. *N. Engl. J. Med.* **365**, 725–733 (2011).
47. Gardner, T. J. et al. Targeted cellular micropharmacies: cells engineered for localized drug delivery. *Cancers* **12**, 2175 (2020).
48. Quintarelli, C. et al. Co-expression of cytokine and suicide genes to enhance the activity and safety of tumor-specific cytotoxic T lymphocytes. *Blood* **110**, 2793–2802 (2007).
49. Garber, K. Driving T-cell immunotherapy to solid tumors. *Nat. Biotechnol.* **36**, 215–219 (2018).

Methods

Chemical synthesis. See Supplementary Note for synthetic methods and analytical data for all new compounds.

Recombinant proteins. CPG2 (ref. [24]) and β-Lac[31] proteins were produced and purified by GenScript. Constructs contain C-terminal hemagglutinin (HA) and His_6 epitope tags and were purified by nickel affinity chromatography.

Cloning and generation of retroviral vectors and cell lines. HEK293T cell lines were generated using retroviral transduction with the MMLV gamma-retroviral vector pLGPW or pLHCX (gifts from the D. Tortorella laboratory, Icahn School of Medicine at Mount Sinai). CAR-T and SEAKER vectors were generated by cloning into the SFG gamma-retroviral vector encoding CD19-directed CAR with human 4-1BB costimulatory element and CD3 zeta chain (SFG-19BBz)[50] or, for the syngeneic mouse model, the vector encoding α-MUC16 (4H11) CAR with murine CD28 costimulatory element and murine CD3 zeta chain (SFG-MUC28z)[16]. β-Lac and CPG2 were cloned upstream of the CAR constructs and separated by a P2A self-cleaving sequence. Standard molecular biology techniques and Gibson assembly were used to generate all constructs. Retroviral producer lines were generated with $CaCl_2$ (Promega) to transiently transfect H29 cells with retroviral constructs encoding CARs or SEAKERs. Supernatant from the H29 cells was collected and used to transduce 293Glv9, PG13 or Phoenix-Eco stable packaging cells. Individual producers were subcloned and expanded.

Cell culture. Cells were maintained in Roswell Park Memorial Institute (RPMI) medium supplemented with 10% FBS, 2 mM L-glutamine, 100 IU ml^{-1} penicillin, 100 μg ml^{-1} nonessential amino acids, sodium pyruvate and *N*-2-hydroxyethylpiperazine-*N*-2-ethane sulfonic acid (HEPES). Human T cell media was supplemented with 100 IU ml^{-1} IL-2.

T cell isolation and modification. Peripheral blood mononuclear cells were isolated from healthy donors. Peripheral blood mononuclear cells were activated with 50 ng ml^{-1} OKT-3 antibody (MACS) and 100 IU ml^{-1} IL-2 for 2 days before transduction and maintained in 100 IU ml^{-1} thereafter. Trandsuction was performed by centrifugation of activated T cells in media from retroviral producers at 2,000*g* at room temperature for 1 h on RetroNectin-coated plates (TakaraBio) for two consecutive days. Experiments were performed in compliance with all relevant ethical regulations and in accordance with Memorial Sloan Kettering (MSK) IRB Protocol 00009377.

Mouse T cells were engineered as previously described[16]. In brief, T cells were isolated from spleens of naive mice by mechanical disruption using a 100-μm cell strainer. Splenocytes were collected and red blood cells were lysed with ammonium-chloride-potassium lysing buffer (ThermoFisher A1049201). Splenocytes were activated overnight with CD3/CD28 Dynabeads (Life Technologies) and 50 IU ml^{-1} human IL-2. Activated T cells were transduced by centrifugation with retroviral supernatant from transduced Phoenix-Eco cells on RetroNectin-coated plates (TakaraBio) for two consecutive days.

Flow cytometry. Transduction efficiency was determined by flow cytometry using an Alexa647-labeled anti-idiotype antibody directed to the CD19-targeted CAR (mAb clone no. 19E3, generated at MSK Antibody and Bioresource Core Facility) or a phycoerythrin (PE)-conjugated rabbit antibody directed to the myc epitope tag in the MUC16-targeted CAR (Cell Signaling Technology 64025S). The following additional commercial antibodies were used in flow cytometry experiments where specified: Alexa647-anti-HA (ThermoFisher 26183-A647, clone 26187), APC-CD19 (BD 555415), PE-CD69 (BioLegend 310906) and APC/Cy70-CD3 (BioLegend UCHT1). All samples were washed and stained in fluorescence-activated cell sorting buffer (2% FBS in PBS) at 4 °C. Data were collected using a Guava EasyCyte HT flow cytometer (Millipore) or an LSR Fortessa (BD). FlowJo software was used for all data analyses.

Immunoprecipitation and western blot analysis. Anti-HA agarose beads (ThermoFisher 26181) were incubated with cell supernatant or mouse ascites for 2 h at 4 °C on a nutator. The beads were washed twice with cold PBS, and Laemmli sample buffer (BioRad 161-0747) with or without β-mercaptoethanol was added. Protein samples (immunoprecipitate or total cell lysates) were homogenized and heated three times for 3 min at 95 °C and resolved by SDS–PAGE. Gels were transferred to nitrocellulose membranes and blotted for respective antibodies in tris-buffered saline with Tween 20 (ThermoFisher 28360). Detection of antibody was achieved with Pierce ECL femto western substrate (ThermoFisher 34095). The following antibodies were used for immunoblot: mouse IgG-HRP-conjugated antibody (R&D systems HAF007), rabbit IgG-HRP-conjugated antibody (R&D systems HAF008), anti-HA (Invitrogen 26183). Polyclonal anti-CPG2 and anti-β-Lac antibodies were raised in rabbits by inoculation with whole recombinant protein produced in *Escherichia coli* and purified by nickel bead affinity chromatography (service performed by GenScript).

Enzyme-linked immunosorbent assay (ELISA) analysis. Sandwich ELISAs were performed on 96-well Immulon HBX plates (ThermoFisher). A mouse IgG anti-HA antibody was used to capture protein (Invitrogen 26183) and a polyclonal mouse antirabbit HRP antibody was used as detection antibody (R&D systems HAF008). Protein was detected using TMB (3,3′,5,5′-tetramethylbenzidine) substrate (ThermoFisher 34028) and H_2SO_4 acid quench, and read on a SpectraMax M2 plate reader (Molecular Devices). Data were analyzed with SoftMax Pro software.

CPG2 glutamate release assay. Recombinant CPG2 enzyme was incubated with glutamate prodrugs in CPG2 reaction buffer (1 M Tris·HCl, 2 mM $ZnCl_2$) for 2 h at 37 °C and the enzyme/prodrug mixture was combined 1:1 with Amplex Red Glutamate Oxidase Assay mixture (ThermoFisher A12221). Following 30 min at 37 °C, fluorescent emission at 590 nm was measured on a SpectraMax M2 plate reader (Molecular Devices). Data were analyzed with SoftMax Pro software.

CPG2 methotrexate cleavage assay. Methotrexate (Accord Healthcare) was incubated at a final concentration of 450 μM with recombinant CPG2 enzyme, CAR-T cells, or cell supernatant and incubated at 37 °C for 16 h. Absorbance at 390 nm was recorded on a NanoDrop spectrophotometer (Thermo Scientific).

β-Lac nitrocefin cleavage assay. Cell supernatant, mouse ascites or mouse blood was serially diluted (twofold) and mixed 1:1 with 0.2 mM nitrocefin (abcam ab145625). Samples were incubated 1–16 h at room temperature and absorbance at 490 nm was read on a SpectraMax M2 plate reader (Molecular Devices). Data were analyzed with SoftMax Pro software.

Enzyme kinetic assays. Analysis of enzyme kinetics reported in Supplementary Table 2 was performed on an automated SPE RapidFire-MS, equipped with a 6520 TOF accurate mass spectrometer detection system (Agilent Technologies). The 6520 TOF–MS has a theoretical limit of high-femtogram sensitivity and up to five orders of magnitude dynamic range. This instrument also includes a Zymark Twister robotic arm that handles microtiter plates, and a SPE purification system. Samples were aspirated from each well of a 384-well microtiter plate and injected onto a C18 SPE cartridge (catalog no. G9205A) for detection of APdMG-Glu (**7**), Ceph-AMS (**3**) and nitrocefin, or a graphitic carbon SPE cartridge (catalog no. G9206A) for detection of AMS (**1**) and methotrexate. Cartridges were washed and eluted with solvent system A or B (below) onto the electrospray MS, where the mass spectra were collected in positive mode (Ceph-AMS, APdMG-Glu, nitrocefin) or negative mode (AMS, methotrexate). The RapidFire sipper was washed between sample injections using alkaline/organic and aqueous alkaline solvents. RapidFire-MS screening data were processed and analyzed using Agilent MassHunter Software.

Solvent system A (for detection of AMS, APdMG-Glu, Ceph-AMS and nitrocefin): washed with aqueous alkaline buffer (10 mM ammonium acetate, pH 10) and eluted using an alkaline/organic solvent (50% methanol + 50% isopropanol in 2 mM ammonium acetate and 0.1% formic acid).

Solvent system B (for detection of methotrexate) was as follows: washed with aqueous alkaline buffer (5 mM ammonium acetate, pH 10) and eluted using an alkaline/organic solvent (50% water + 25% acetonitrile + 25% acetone in 5 mM ammonium acetate, pH 10).

Analyte, reaction time, aliquot frequency, exact mass and *m/z* detected were: AMS, 10 min, 1 min, 346.0696, 345.0659 $[M+H]^+$; ApDMG-Glu, 180 s, 20 s, 698.1903, 699.2136 $[M+H]^+$; methotrexate, 180 s, 20 s, 454.1713, 453.168 $[M+H]^+$; Ceph-AMS, 90 min, 10 min, 682.0934, 683.1068 $[M+H]^+$ and nitrocefin, 270 s, 30 s, 516.4990, 539.0262 $[M+Na]^+$.

For AMS-Glu (**2**), CPG2 (752 nM) was incubated with various concentrations of AMS-Glu (**2**) (25–200 μM) at 22 °C in PBS in a glass vial. Aliquots were removed at various time points (up to 10 min) and added to a 384-well plate containing 2 volumes of 0.1% formic acid to stop the reaction. AMS (**1**) product formation was measured by RapidFire-MS. The resulting data were fitted to the Michaelis–Menten equation to determine the Michaelis constants.

For APdMG-Glu (**7**), CPG2 (752 nM) was incubated with various concentrations of APdMG-Glu (**7**) (12.5–100 μM) at 22 °C in PBS in a glass vial. Aliquots were removed at various time points (up to 3 min) and added to a 384-well plate containing 6 volumes of 0.1% formic acid to stop the reaction. APdMG-Glu (**7**) substrate depletion was measured by RapidFire-MS. The resulting data were fitted to the Michaelis–Menten equation to determine the Michaelis constants.

For methotrexate, CPG2 (37.6 nM) was incubated with various concentrations of methotrexate (25–200 μM) at 22 °C in PBS in a glass vial. Aliquots were removed at various time points (up to 3 min) and added to a 384-well plate containing 2 volumes of 0.1% formic acid to stop the reaction. Methotrexate substrate consumption was measured by RapidFire-MS. The resulting data were fitted to the Michaelis–Menten equation to determine the Michaelis constants.

For Ceph-AMS (**3**) and nitrocefin, β-Lac (11.44 nM) was incubated with various concentrations of Ceph-AMS (**3**) or nitrocefin (25–200 μM) at 22 °C in PBS in a glass vial. Aliquots were removed at various time points (up to 90 min for Ceph-AMS or 4.5 min for nitrocefin) and added to a 384-well plate containing 2 volumes of 0.1% formic acid to stop the reaction. Substrate consumption was measured by RapidFire-MS. The resulting data were fitted to the Michaelis–Menten equation to determine the Michaelis constants.

Cytotoxicity assays. Prodrug/drug IC_{50} and *trans*-cytotoxicity and *cis*-cytotoxicity assays with secreted enzymes were performed using CellTiter-Glo (Promega). Cells were analyzed in triplicate wells of a 96-well dish and equivalent volume of CellTiter-Glo reagent was added to each well. Following a 10-min incubation at room temperature, samples were transferred to White 96-well Optiplates (Perkin Elmer) and luminescence was measured on a SpectraMax M2 plate reader (Molecular Devices). Data were analyzed with SoftMax Pro software.

The cytotoxicity of CAR-T cells and SEAKER cells was determined by luciferase-based assays. Target cells (Raji and SKOV-3) expressing firefly luciferase and GFP (fLuc-GFP) were used. Effector and tumor target cells were cocultured in triplicate at the indicated E:T ratio using clear bottom, white 96-well assay plates (Corning 3903) with 5×10^4 target cells in a total volume of 200 µl. Target cells alone were plated at the same cell density to determine maximum luciferase activity. Cells were cocultured for 4–18 h, at which time D-luciferin substrate (Gold Biotech LUCK) was added at a final concentration of 0.5 µg µl^{-1} to each well. Emitted light was detected in a Wallac EnVision Multilabel reader (Perkin Elmer). Target lysis was determined as $(1-(RLU_{sample})/(RLU_{max}))\times100$ (RLU, relative light unit).

Mixed cell bystander toxicity assays were performed by incubating untransduced T cells or SEAKER cells with Raji and SET2 cells at 4:1:1 (CAR-T cells:Raji:SET2) ratio. Following 24 h of coculture, prodrug was added and cells were cultured for an additional 48 h before analysis by flow cytometry. Detection of GFP and anti-CD19 staining (APC-CD19 (BD 555415)) delineated Raji versus SET2 versus CAR-T cells. Cell count was measured by acquiring cells for 30 s per well on a Guava EasyCyte flow cytometer, and multiplying the percentage of respective gates by the total cells acquired.

gLuc-19BBz reporter CAR-T cell analysis in vitro. Assays measuring proliferation of gLuc-19BBz CAR-T cells were performed by measuring emitted light following cleavage of coelenterazine substrate (Prolume 3032). Cells were cocultured for 4–18 h, at which time coelenterazine was added at a final concentration of 2.5 µM to each well. Emitted light was detected in a Wallac EnVision Multilabel reader (Perkin Elmer).

Pharmacological assays and pharmacokinetic studies. In vitro pharmacological assays and mouse pharmacokinetic studies were carried out by Sai Life Sciences, Hyderabad, India, in compliance with all relevant ethical regulations and in accordance with Institutional Animal Ethics Committee (IAEC) protocols FB-18-022 and FB-19-033. Plasma protein binding studies were carried out by rapid equilibrium dialysis (ThermoFisher) using fresh plasma from NOD-SCID mice (ACTREC) or human drug-free volunteers (Bhonsle's Laboratory, Mumbai, India) and LC–MS/MS analysis. Plasma stability studies were carried out in fresh plasma from NOD-SCID mice (ACTREC), or from human drug-free volunteers (AJ Medical) by LC–MS/MS analysis. Microsomal stability studies were carried out in pooled liver microsomes from CD-1 mice (Gibco) or humans (BD Gentest) by LC–MS/MS analysis. Single-dose pharmacokinetic studies were carried out by i.p. injection of NOD-SCID mice ($n=9$) and LC–MS/MS analysis of plasma samples at 0.08, 0.25, 0.5, 1, 2, 4, 8, 12 and 24 h ($n=3$ per timepoint). Pharmacokinetic parameters were calculated using the noncompartmental analysis tool of Phoenix WinNonlin.

Mouse efficacy studies. All experiments were performed in compliance with all relevant ethical regulations and in accordance with MSK IACUC protocol 96-11-044.

Intraperitoneal (i.p.) model. NSG mice (NOD.Cg-Prkdcscid Il2rgtm1Wjl/SzJ, 7–13 weeks old, male and female) were obtained from the Jackson Laboratory. Mice were engrafted on day 0 with 0.5×10^6 Raji-eGFP/fLuc tumor cells (i.p.) and treated on day 2 with 0.5×10^6 CAR-T or SEAKER cells (i.p.). For enzyme activity studies, ascites and peripheral blood samples were taken on day 4. For efficacy studies, prodrug was administered beginning on day 4. For prodrug retreatment studies, Ceph-AMS (**3**) was administered again beginning on day 22 posttumor engraftment (4 mg kg^{-1}, i.p., b.i.d. for three doses). For enzyme persistence studies, SEAKER cells were extracted on day 30 posttumor engraftment and analyzed for exhaustion markers and β-Lac enzyme activity.

For the mixed antigen-positive/negative tumor model, a total of 2×10^6 Nalm6 cells were engrafted on day 0 (1:1 Nalm6-gLuc (CD19$^+$/mCherry$^+$/*Gaussia* luciferase$^+$) and Nalm6-fLuc (CD19$^-$/eGFP$^+$/firefly luciferase$^+$)). Mice were treated on day 10 with 1×10^6 CAR-T or SEAKER cells (i.p.), and Ceph-AMS prodrug (**3**) was administered on day 14 (4 mg kg^{-1} i.p., b.i.d. for three total doses).

For enzyme persistence studies, SEAKER cells were extracted on day 30 posttumor engraftment by injection of 3 ml of PBS directly into the peritoneum, followed by gentle agitation and withdrawal using a syringe. Cells were centrifuged and analyzed for exhaustion markers and β-Lac enzyme activity.

Subcutaneous model. NSG mice (NOD.Cg-Prkdcscid Il2rgtm1Wjl/SzJ, 7–13 weeks old, male and female) were obtained from the Jackson Laboratory. Mice were engrafted on day 0 with 1×10^6 Raji-eGFP/fLuc cells (1:1 with Matrigel, ThermoFisher 356234). On day 7, 3×10^6 CAR-T or SEAKER cells were injected in the tail vein. For enzyme activity studies, tumors were resected on day 16 and analyzed. For efficacy studies, prodrug was administered beginning on day 15 (AMS-Glu (**2**): 50 mg kg^{-1}, i.p., b.i.d. on days 15–20 posttumor engraftment); (Ceph-AMS (**3**): 4 mg kg^{-1} i.p., b.i.d. on days 15, 17 and 19 posttumor engraftment).

Syngeneic model. C57BL/6 mice (7–13 weeks old, male and female) were obtained from the Jackson Laboratory. Mice were engrafted on day 0 with 3×10^6 ID8 tumor cells (i.p.). On day 20, tumor-bearing mice were preconditioned with 100 mg kg^{-1} cyclophosphamide to improve adoptive T cell engraftment, then on day 21, 3×10^6 β-Lac-MUC28z SEAKER cells were engrafted (i.p.). On day 28, mice were euthanized and a peritoneal lavage was performed using 3 ml of PBS per mouse.

For SEAKER cell persistence studies, recovered cells were washed and centrifuged in PBS, then stained with a Myc-Tag (71D10) rabbit mAb (PE conjugate) (Cell Signaling Technology 64025) to detect CAR expression.

For enzyme persistence studies, recovered cells were lysed on dry ice and soluble proteins were dissolved in PBS, then analyzed in the nitrocefin assay above.

For ex vivo immunogenicity assays, sera were collected from the mice in a separate experiment at the indicated time points by cheek bleed, followed by clotting and centrifugation of whole blood. Recombinant β-Lac was coated onto an ELISA plate at 100 ng ml^{-1} in ELISA coating buffer (0.05 M carbonate-bicarbonate, pH 9.6). Collected sera were incubated on the coated plates for 1 h. After washing, goat α-mouse IgG-HRP was incubated in each well, followed by development with TMB substrate and stopping with H_2SO_4. Absorbance at 450 nm was read on a SpectraMax M2 plate reader (Molecular Devices). Data were analyzed with SoftMax Pro software.

Immunohistochemistry. The immunohistochemistry detection of β-Lac was performed at MSK Molecular Cytology Core Facility, using a Discovery XT processor (Ventana Medical Systems). A rabbit β-Lac antibody was used in 6 µg ml^{-1} concentration. The incubation with the primary antibody was done for 5 h, followed by 60 min incubation with biotinylated goat antirabbit IgG (Vector Laboratories, catalog no. PK6101) in 5.75 µg ml^{-1}, Blocker D, Streptavidin-HRP and DAB detection kit (Ventana Medical Systems) were used according to the manufacturer's instructions. Slides were counterstained with hematoxylin and coverslipped with Permount (Fisher Scientific).

CRISPR–Cas9 knockout of CD19. Nalm6–GFP$^+$/firefly luciferase$^+$/CD19-knockout cells were generated by transduction of Nalm6-GFP$^+$/firefly luciferase$^+$ cells with LentiCRISPRv2 (Addgene plasmid 52961)[51] encoding a sgRNA targeting CD19 (CCCCATGGAAGTCAGGCCCG). Successful knockout was confirmed by flow cytometry and CD19-negative cells were fluorescence-activated cell sorting sorted to >97% purity.

Bioluminescent imaging. Bioluminescent tumor imaging was performed using a Xenogen IVIS imaging system with Living Image software (Xenogen Biosciences). Image acquisition was done on a 25-cm field of view at medium binning level at various exposure times. Coelenterazine (100 µg) was administered i.p. for gLuc-CAR-T studies, or via retro-orbital injection for s.c. tumor studies. D-Luciferin (3 µg) was administered i.p. for firefly luciferase tumor imaging. Images in a single data set were normalized together according to color intensity as indicated by a scale bar.

Statistical analysis. The log-rank (Mantel–Cox) and Student's *t*-tests (two-tailed) were performed using GraphPad Prism where appropriate. Statistical significance was indicated accordingly: $^*P<0.05$, $^{**}P<0.01$, $^{***}P<0.001$. For all technical replicates reported, measurements were taken from distinct samples.

Reporting Summary. Further information on research design is available in the Nature Research Reporting Summary linked to this article.

Data availability

The authors declare that the data supporting the findings of this study are available within the article and its Supplementary Information files. Any raw data not provided therein are available from the corresponding authors upon reasonable request.

References

50. Riviere, I., Brose, K. & Mulligan, R. C. Effects of retroviral vector design on expression of human adenosine deaminase in murine bone marrow transplant recipients engrafted with genetically modified cells. *Proc. Natl Acad. Sci. USA* **92**, 6733–6737 (1995).
51. Sanjana, N. E., Shalem, O. & Zhang, F. Improved vectors and genome-wide libraries for CRISPR screening. *Nat. Methods* **11**, 783–784 (2014).

Acknowledgements

We thank E. de Stanchina and C. Hagen (MSK Antitumor Assessment Core Facility) for assistance with mouse toxicology studies, G. Sukenick and R. Wang (MSK Analytical NMR Core Facility) for expert nuclear magnetic resonance and mass spectral support, J.

Fraser Glickman and C. Adura Alcaino (Rockefeller High-Throughput and Spectroscopy Resource Center) for assistance with SPE–MS experiments, G. Chiosis and S. Sharma (MSK) for assistance with LC–MS/MS experiments and B. Yoo (MSK) for helpful discussions on the synthesis of APdMG-Glu. Financial support from the NIH (grant nos. P01 CA023766 to D.A.S. and D.S.T., R01 CA55349 and R35 CA241894 to D.A.S., R01 AI118224 to D.S.T. and CCSG P30 CA008748 to C.B. Thompson), the Tudor Fund (to D.A.S.), the Lymphoma Fund (to D.A.S.), the Commonwealth Foundation and MSK Center for Experimental Therapeutics (to D.A.S. and D.S.T.) is gratefully acknowledged.

Author contributions

T.J.G., C.M.B. and D.A.S. conceived the in vitro and in vivo experiments with technical advice from D.W. and R.J.B. T.J.G. and C.M.B. executed the in vitro and in vivo experiments with assistance from K.G.K., M.M.D., A.Y.C. and G.M. J.P.L., N.K., B.C.C. and D.S.T. conceived the chemical, biochemical and ADME-PK experiments. J.P.L., B.C.C. and K.M.N. carried out the chemical syntheses. J.P.L., N.K. and B.C.C. carried out the biochemical assays. T.J.G., J.P.L., C.M.B., D.S.T. and D.A.S. wrote the paper with input from all coauthors.

Competing interests

D.A.S., D.S.T. and R.J.B. are consultants for, have equity in and have sponsored research agreements with CoImmune, which has licensed technology described in this paper from MSK. D.A.S. has equity in or is a consultant for: Actinium Pharmaceuticals, Arvinas, Eureka Therapeutics, Iovance Biotherapeutics, OncoPep, Pfizer, Repretoire and Sellas. D.S.T. has been a consultant and/or paid speaker for Eli Lilly, Elsevier, Emerson Collective, Merck, National Institutes of Health, Venenum Biodesign, the Research Center for Molecular Medicine of the Austrian Academy of Sciences and the Institute for Research in Biomedicine, Barcelona. R.J.B. is a cofounder and receives royalties from Juno Therapeutics/Celgene. MSK has filed for patent protection behalf of T.J.G., J.P.L., D.S.T. and D.A.S. for inventions described in this paper. The remaining authors declare no competing interests.

Additional information

Extended data are available for this paper at https://doi.org/10.1038/s41589-021-00932-1.

Supplementary information The online version contains supplementary material available at https://doi.org/10.1038/s41589-021-00932-1.

Correspondence and requests for materials should be addressed to Derek S. Tan or David A. Scheinberg.

Peer review information *Nature Chemical Biology* thanks Yuan Gao and the other, anonymous, reviewer(s) for their contribution to the peer review of this work.

Reprints and permissions information is available at www.nature.com/reprints.

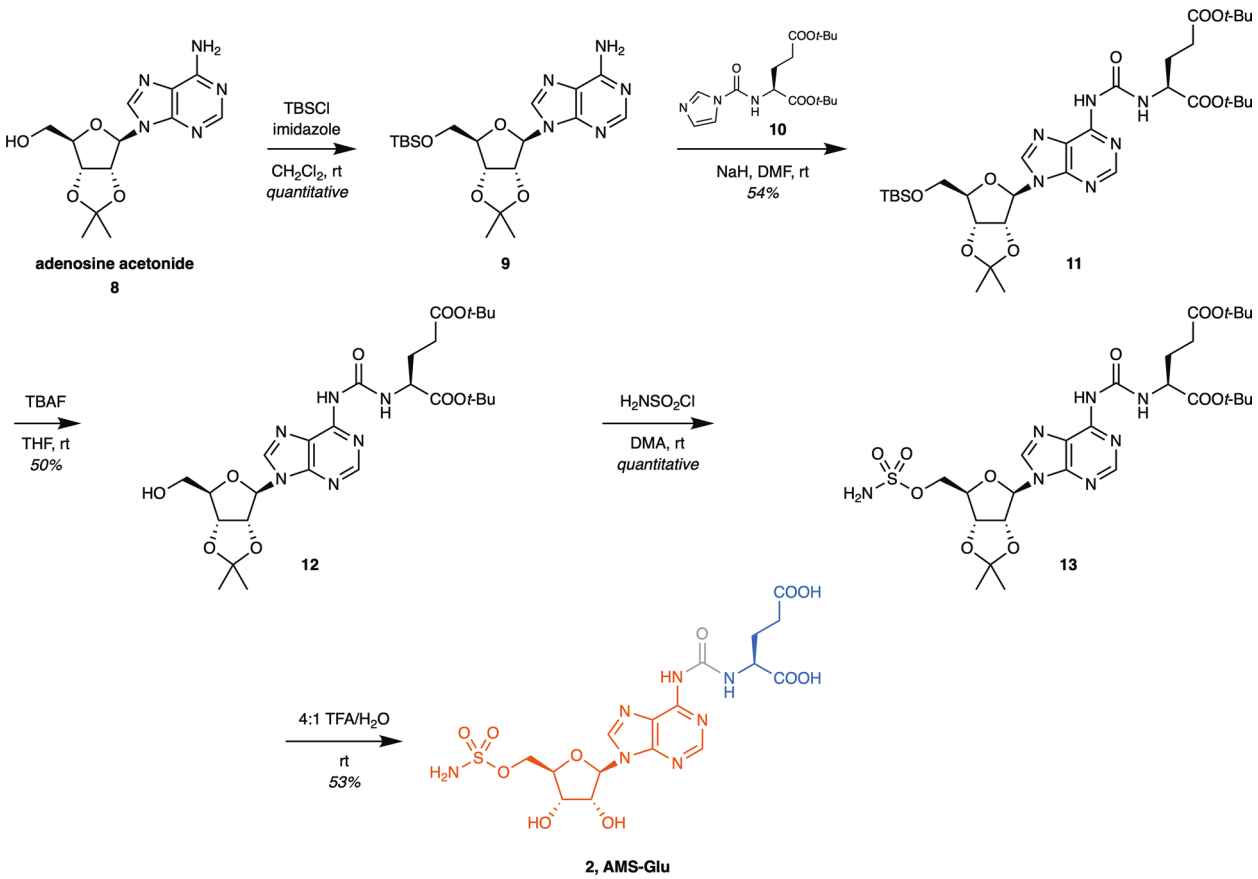

Extended Data Fig. 1 | Synthesis of AMS-Glu prodrug (2). DMA = *N*,*N*-dimethylacetamide; DMF = *N*,*N*-dimethylformamide; TBAF = tetrabutylammonium fluoride; TBS = t-butyldimethylsilyl.

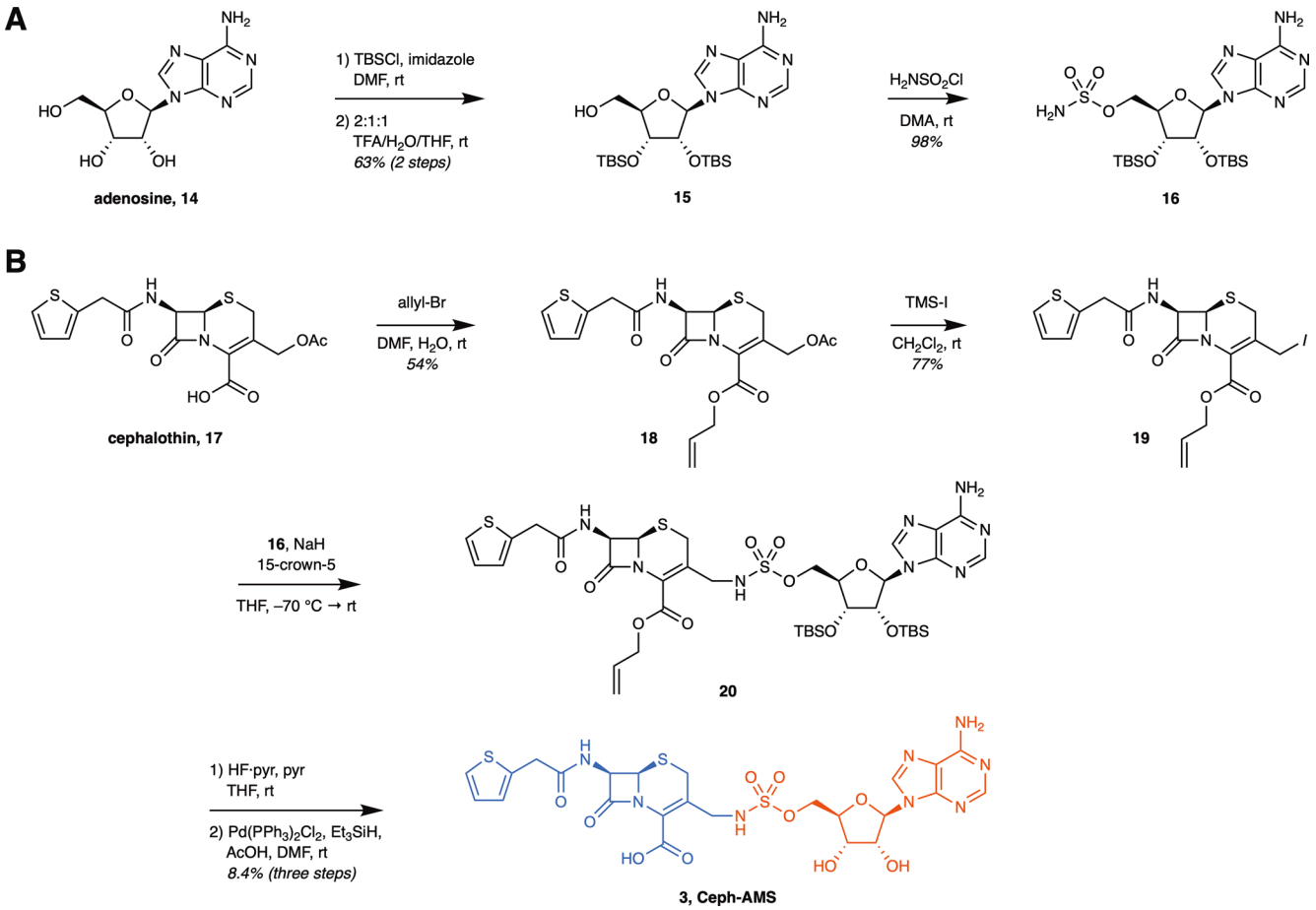

Extended Data Fig. 2 | Synthesis of Ceph-AMS prodrug (3). (a) Synthesis of protected AMS precursor **16**. **(b)** Synthesis of Ceph-AMS (**3**). pyr = pyridine; TFA = trifluoroacetic acid; THF = tetrahydrofuran; TMS = trimethylsilyl.

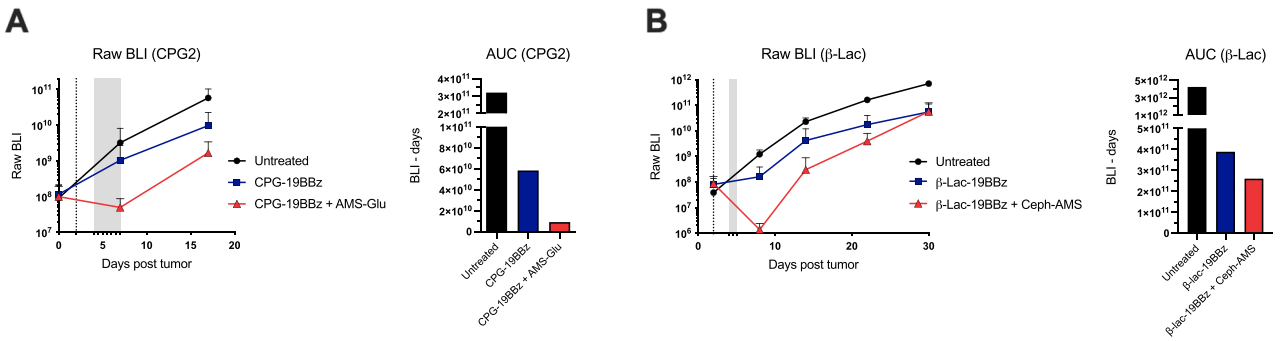

Extended Data Fig. 3 | Complete bioluminescent imaging data for *in vivo* efficacy in mouse intraperitoneal Raji tumor xenografts. Mice treated with **(a)** CPG2-19BBz SEAKER cells and AMS-Glu (**2**) (50 mg/kg, *ip*, *bid*, days 2-7 post-CAR engraftment, 12 doses total, gray band) or **(b)** β-Lac-19BBz SEAKER cells and Ceph-AMS (**3**) (4 mg/kg, *ip*, *bid*, days 2–3 post-CAR engraftment, 3 doses total, gray band). Raw BLI is plotted on log scale; AUC is plotted on split linear scale. (mean ± s.d. of n = 5 mice per group; experiment was repeated with similar results.) Representative images are shown in Fig. 5d and e, respectively, of the manuscript.

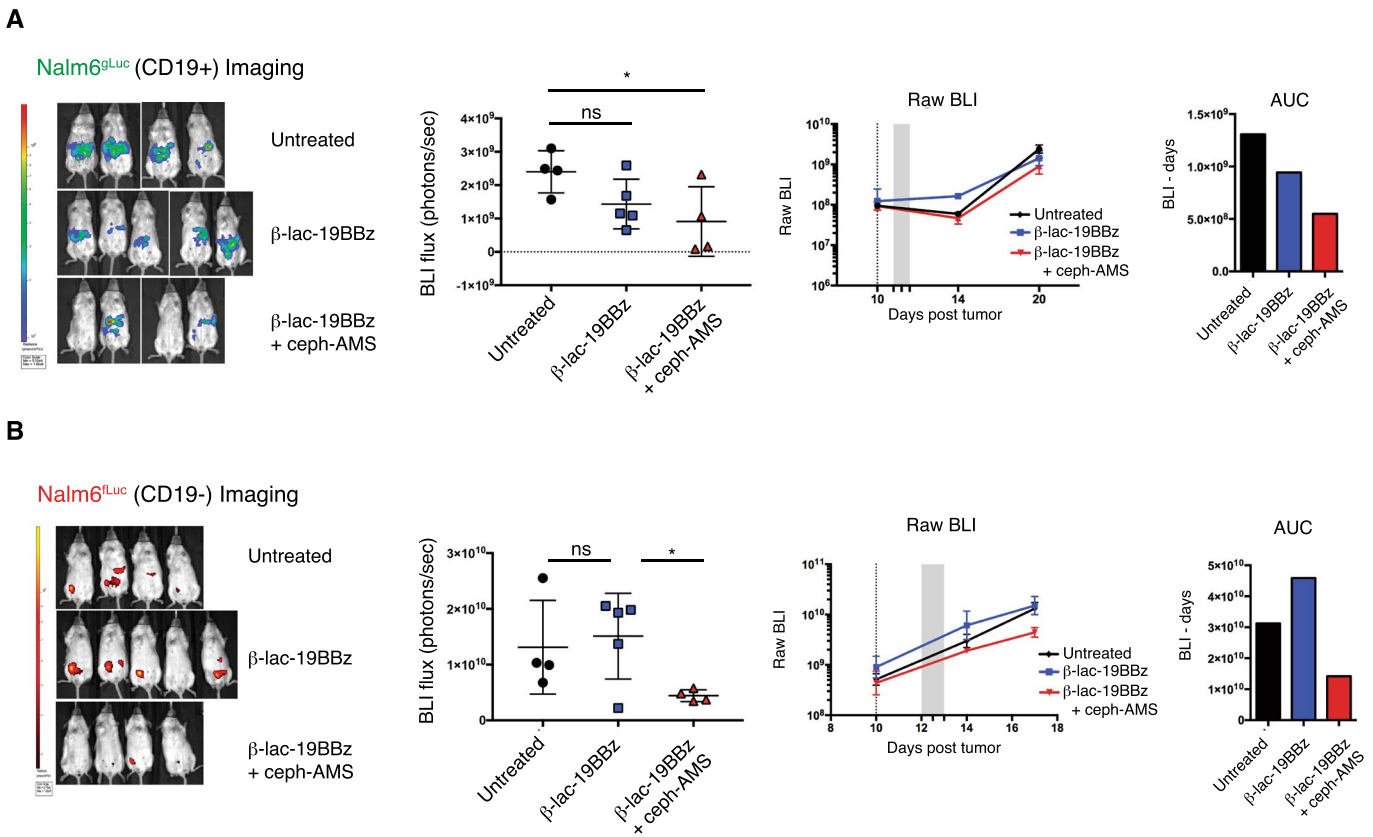

Extended Data Fig. 4 | Complete bioluminescent imaging data for *in vivo* efficacy against antigen-negative cells in intraperitoneal heterogeneous tumor xenografts. (a) Bioluminescent imaging (BLI) and quantification of CD19⁺ Nalm6 cells expressing mCherry and *Gaussia* luciferase (Nalm6-mCherry/gLuc [CD19⁺]) in untreated mice or mice receiving β-Lac-19BBz SEAKER cells plus or minus 3 injections of Ceph-AMS (**3**: 4 mg/kg, *ip*, *bid*). Images taken at day 20 post tumor engraftment; one mouse in the group treated with SEAKER cells and prodrug showed tumor clearance but died after day 14 and is omitted. Complete radiance data is shown in the right two panels, with raw BLI plotted on log scale and AUC plotted on a linear scale. (Mean ± s.d. of n = 4 (untreated, SEAKER + prodrug) or n = 5 (SEAKER alone) mice per group; Student's two-tailed *t*-test: ns = not significant; $^*p < 0.05$; experiment was performed once). **(b)** BLI and quantification of CD19⁻ Nalm6 cells expressing eGFP and firefly luciferase (Nalm6-eGFP/fLuc [CD19⁻]) in untreated mice or mice receiving β-Lac-19BBz SEAKER cells plus or minus 3 injections of Ceph-AMS (**3**: 4 mg/kg, *ip*, *bid*). Images taken at day 17 post tumor engraftment; one mouse in the group treated with SEAKER cells and prodrug died after day 14 and is omitted. The left two panels also appear in Fig. 5g,h of the manuscript. Complete radiance data is shown in the right two panels, with raw BLI plotted on log scale and AUC plotted on a linear scale. (Mean ± s.d. of n = 4 (untreated, SEAKER + prodrug) or n = 5 (SEAKER alone) mice per group; Student's two-tailed *t*-test: ns = not significant; $^*p < 0.05$; experiment was performed once).

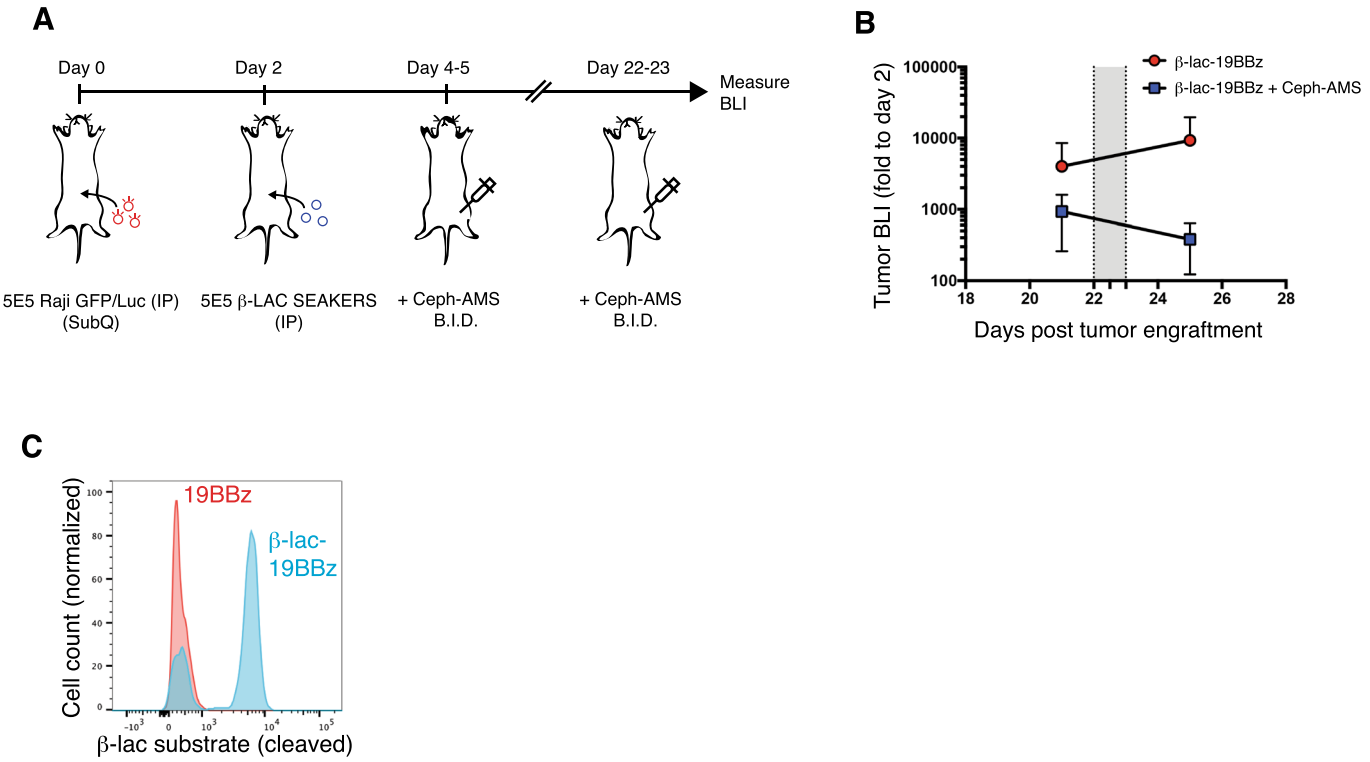

Extended Data Fig. 5 | Persistence of β-Lac enzyme activity and Ceph-AMS prodrug activation in mouse intraperitoneal Raji tumor xenografts after SEAKER cell exhaustion *in vivo*. (a) Experimental scheme for rescue of relapsed Raji xenograft by treatment with Ceph-AMS (**3**: 4 mg/kg, *ip*, *bid*, days 4–5, 3 doses total, then days 22–23 (gray bar), 3 doses total) after exhaustion of β-Lac-19BBz SEAKER cells. **(b)** Quantitation of tumor bioluminescence before and after second dosing period (median with s.d. of n = 4 mice per group; experiment was performed once). **(c)** Persistence of β-Lac enzyme activity in β-Lac-19BBz SEAKER cells extracted from two of the mice from the experiment in panel **a** at day 30 (day 28 post administration), in comparison to standard 19BBz CAR-T cell controls (flow cytometry analysis: β-Lac substrate = CCF2-AM).

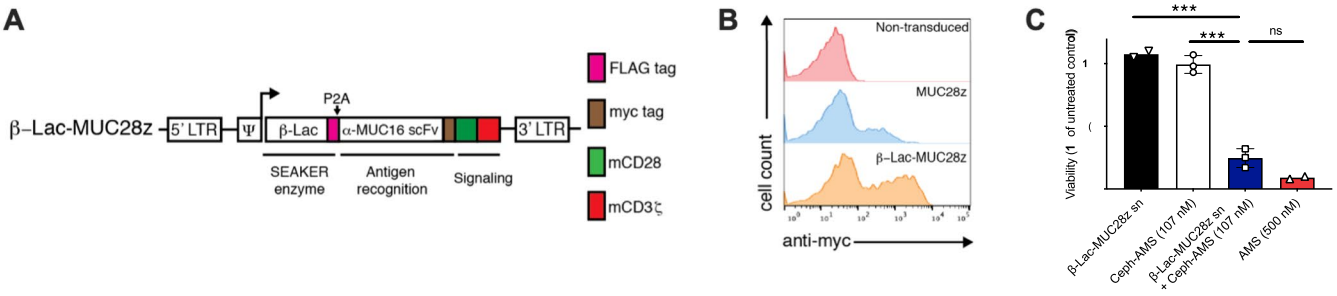

Extended Data Fig. 6 | Construction and characterization of β-Lac-expressing murine SEAKER cells. (a) SEAKER construct encoding secreted β-Lac and a murine CAR: β-Lac-MUC28z (β-Lac/α-MUC16/CD28/CD3ζ). LTR = long terminal, Ψ = psi packaging element, FLAG = FLAG epitope tag (pink), P2A = 2A self cleaving peptide, α-MUC16 scFv = MUC-16-specific mouse-derived single chain variable fragment, myc = Myc epitope tag (brown), mCD28 = mouse CD28 costimulatory domain (green), mCD3ζ = mouse CD3 zeta chain (red). **(b)** Flow cytometry analysis of α-MUC16 CAR expression in retrovirally-transduced primary mouse T cells (fluorescently (phycoerythrin, PE) labeled anti-idiotype antibody; representative data from 5 independent experiments). **(c)** Trans-cytotoxicity of supernatant fluid (sn) from β-Lac-MUC28z SEAKER cells with or without Ceph-AMS (**3**: 107 nM) against mouse EL4 lymphoma cells, compared to prodrug alone and parent drug AMS (**1**: 500 nM) (24 h, CellTiter-Glo assay; mean ± s.d. of n = 3 technical replicates; Student's two-tailed *t*-test: ns = not significant, ***$p < 0.001$; experiment was perfomed once).

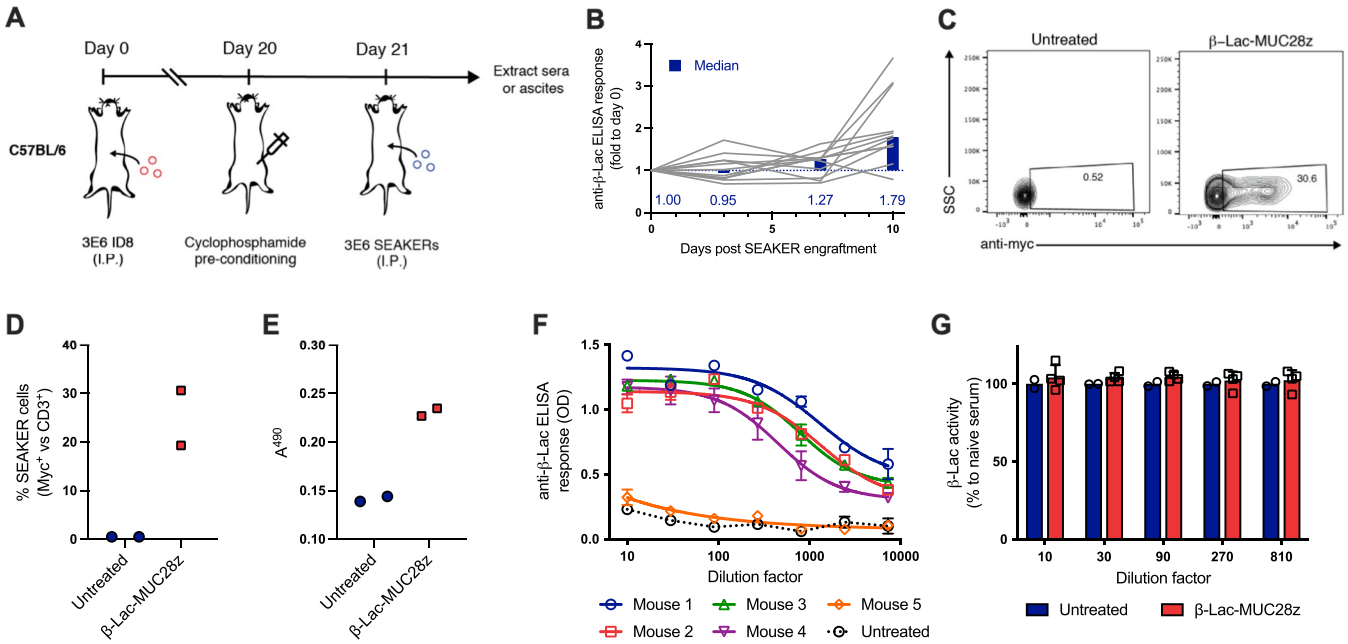

Extended Data Fig. 7 | Assessment of SEAKER cell immunogenicity in an immunocompetent mouse model. Assessment of SEAKER cell immunogenicity in an immunocompetent mouse model. **(a)** Experimental scheme to assess immunogenicity of β-Lac-MUC28z SEAKER cells in a syngeneic intraperitoneal ID8 tumor model. Sera were collected on Days 21, 24, 28, and 31 and tested for anti-β-Lac antibodies in panel **b**. In a separate experiment, ascites were recovered on Day 28 by peritoneal lavage and tested for the presence of SEAKER cells in panels **c,d** and β-Lac enzyme activity in panel **e**. **(b)** Detection anti-β-Lac antibodies in sera over 10 days following SEAKER cell engraftment (Days 21–31) (median with lines representing each individual mouse of n = 12; experiment was performed once). **(c,d)** Flow cytometry analysis of SEAKER cell (myc^+) persistence among T cells ($CD3^+$) and **(e)** nitrocefin cleavage-based quantitation of β-Lac enzyme activity in ascites recovered 7 days after SEAKER cell engraftment (Day 28) (representative data shown from n = 2 mice per group; on average, 25% of T cells were SEAKER-positive; experiment was performed once). SSC = side scatter. **(f)** In a third experiment, mice were treated as in panel **a**, but without cyclophosphamide pretreatment to maximize the antibody response, then sera were recovered 5 days after SEAKER cell engraftment (Day 26) and analyzed for anti-β-Lac antibodies (n = 1 mouse in untreated group; n = 5 mice in treated group; mean ± s.d. of n = 3 technical replicates from each mouse; experiment was performed once). Sera from the 4 mice showing anti-β-Lac antibodies were used for the *ex vivo* enzyme activity experiment in panel **g**. **(g)** Nitrocefin cleavage-based quantitation of enzyme activity of recombinant β-Lac treated with sera from untreated or SEAKER-treated mice from panel **f** (n = 2 mice in untreated group; mean ± s.d. of n = 4 mice in treated group; experiment was performed once).

nature research

Corresponding author(s): Derek Tan, David Scheinberg

Last updated by author(s): 10/05/2021

Reporting Summary

Nature Research wishes to improve the reproducibility of the work that we publish. This form provides structure for consistency and transparency in reporting. For further information on Nature Research policies, see our Editorial Policies and the Editorial Policy Checklist.

Statistics

For all statistical analyses, confirm that the following items are present in the figure legend, table legend, main text, or Methods section.

n/a	Confirmed	
☐	☒	The exact sample size (*n*) for each experimental group/condition, given as a discrete number and unit of measurement
☐	☒	A statement on whether measurements were taken from distinct samples or whether the same sample was measured repeatedly
☐	☒	The statistical test(s) used AND whether they are one- or two-sided *Only common tests should be described solely by name; describe more complex techniques in the Methods section.*
☐	☒	A description of all covariates tested
☒	☐	A description of any assumptions or corrections, such as tests of normality and adjustment for multiple comparisons
☒	☐	A full description of the statistical parameters including central tendency (e.g. means) or other basic estimates (e.g. regression coefficient) AND variation (e.g. standard deviation) or associated estimates of uncertainty (e.g. confidence intervals)
☒	☐	For null hypothesis testing, the test statistic (e.g. *F*, *t*, *r*) with confidence intervals, effect sizes, degrees of freedom and *P* value noted *Give P values as exact values whenever suitable.*
☒	☐	For Bayesian analysis, information on the choice of priors and Markov chain Monte Carlo settings
☒	☐	For hierarchical and complex designs, identification of the appropriate level for tests and full reporting of outcomes
☒	☐	Estimates of effect sizes (e.g. Cohen's *d*, Pearson's *r*), indicating how they were calculated

Our web collection on statistics for biologists contains articles on many of the points above.

Software and code

Policy information about availability of computer code

Data collection	Softmax Pro Version ? was used for collection of nitrocefin, and ELISA binding curve data.
Data analysis	Graph Pad Prism Version 6.0 was used for all data analysis in the study. Flow cytometry data was analyzed using FlowJo Version 10. Living Image Version _ was used for quantification of BLI data.

For manuscripts utilizing custom algorithms or software that are central to the research but not yet described in published literature, software must be made available to editors and reviewers. We strongly encourage code deposition in a community repository (e.g. GitHub). See the Nature Research guidelines for submitting code & software for further information.

Data

Policy information about availability of data

All manuscripts must include a data availability statement. This statement should provide the following information, where applicable:

- Accession codes, unique identifiers, or web links for publicly available datasets
- A list of figures that have associated raw data
- A description of any restrictions on data availability

The data that support the findings of this study are available from the corresponding author upon reasonable request.

Field-specific reporting

Please select the one below that is the best fit for your research. If you are not sure, read the appropriate sections before making your selection.

☒ Life sciences ☐ Behavioural & social sciences ☐ Ecological, evolutionary & environmental sciences

For a reference copy of the document with all sections, see nature.com/documents/nr-reporting-summary-flat.pdf

Life sciences study design

All studies must disclose on these points even when the disclosure is negative.

Sample size	All experiments were performed in triplicate or otherwise noted. For experiments measuring the function of primary human CAR-T cells, samples from 3 or more donors were examined to account for any donor-to-donor variability. Sample size for in-vivo experiments was determined based on animal housing constraints, feasibility of regular BLI imaging measurements, and availability of prodrug compounds. The sample sizes and experimental replicate studies sufficiently account for variabilty in donor material or tumor engraftment/CAR administration.
Data exclusions	No Data exclusions
Replication	When possible all experiments were replicated 2 or more times using material from diverse blood donors. All replication attempts yielded the same conclusions.
Randomization	In-vivo experimental arms were randomly assigned to cages of up to 5 mice following tumor engraftment. Covariates were controlled for through random allocation of donor material form over 10 donors.
Blinding	Tumor engrafted mice were randomized prior to start of treatment and CAR-T administration was performed by technicians who were blinded to the experimental design, or the main investigator who was not blinded to the experimental conditions. All measurements were made objectively.

Reporting for specific materials, systems and methods

We require information from authors about some types of materials, experimental systems and methods used in many studies. Here, indicate whether each material, system or method listed is relevant to your study. If you are not sure if a list item applies to your research, read the appropriate section before selecting a response.

Materials & experimental systems

n/a	Involved in the study
☐	☒ Antibodies
☐	☒ Eukaryotic cell lines
☒	☐ Palaeontology and archaeology
☐	☒ Animals and other organisms
☐	☒ Human research participants
☒	☐ Clinical data
☒	☐ Dual use research of concern

Methods

n/a	Involved in the study
☒	☐ ChIP-seq
☐	☒ Flow cytometry
☒	☐ MRI-based neuroimaging

Antibodies

Antibodies used	Anti-idiotype antibody directed to the CD19-targeted CAR (mAb clone #19E3 – generated at Memorial Sloan Kettering Cancer, Center Antibody and Bioresource Core Facility); Alexa647-anti-HA (Thermo – clone 26187, cat # 26183-A647); APC-CD19 (BD – cat# 555415); PE-CD69 (BioLegend cat#310906); APC/Cy70-CD3 (BioLegend cat# UCHT1); anti-Ms HRP (R&D systems HAF007), anti-Rb (R&D systems HAF008), anti-HA (Invitrogen cat. 26183). Polyclonal anti-CPG2 and anti-β-Lactamase antibodies were raised in rabbits by inoculation with whole recombinant protein produced in e. Coli and purified by nickel bead affinity chromatography (service performed by GenScript). anti-HA (ELISA) (Invitrogen cat. 26183); polyclonal mouse anti-rabbit HRP antibody (R&D systems HAF008). anti-CD3 (OKT-3) (MACS 130-093-87)
Validation	The primary antibodies were validated with positive controls through various experimental strategies using including western blots, flow cytometry, ELISA, immunohistochemistry, and immunoprecipitation studies. Specifically, anti-CPG2 and anti-B-lac antibodies were validated via staining of purified, recombinant protein as well as secondary staining with anti-idiotype antibodies for validation of immunohistochemistry experiments. Anti-idiotype antibodies targeting CAR binders were validated with negative controls transduced with irrelevant CAR constructs. All other antibodies used in the study are from commercial sources with lot validation. Antibodies used in flow cytometry, western blot, and ELISA experiments were further validated and optimized with dose-titration experiments in which a fixed amount of target was stained with a serial dilution of the antibody in question followed by direct detection or secondary binding/detection with an optimized secondary antibody. Data supporting the validation of the antibodies specifically generated for this study (anti-B-lac and anti-CPG2) are available in the supplemental data.

Eukaryotic cell lines

Policy information about cell lines

Cell line source(s)	HCC827, HEK293t, SKOV-3, Raji, Jurkat, SET2, Nalm6, PC9, PG13 and Phoenix-Eco cells are all available commercially via ATCC. 293Glv9 cells were a gift from the Bentjens lab.
Authentication	All commercial cell lines are validate by the supplier via STR profiling . Viral producer lines were regularly exposed to antibiotic selection to ensure purity.
Mycoplasma contamination	Mycoplasma contamination was regularly tested for throughout the study via PCR and found to be negative
Commonly misidentified lines (See ICLAC register)	None

Animals and other organisms

Policy information about studies involving animals; ARRIVE guidelines recommended for reporting animal research

Laboratory animals	Male and Female NSG mice between 7-13 weeks of age were used
Wild animals	No wild animals were used in the study.
Field-collected samples	No Field-collected samples were used in the study.
Ethics oversight	Ethics oversight by the MSK Institutional Animal Care and Use Committee (protocol 96-11-044).

Note that full information on the approval of the study protocol must also be provided in the manuscript.

Human research participants

Policy information about studies involving human research participants

Population characteristics	Gender, age, and ethnic unbiased group on an IRB protocol; male and female donors aged 21-63.
Recruitment	Only healthy volunteer donors were used. Participants recruited based on healthy volunteers working in or near MSK labs. One source of bias may be the participation of only university/healthcare workers, though this is not expected to affect the observed outcomes in any way.
Ethics oversight	MSKCC IRB, Protool 00009377.

Note that full information on the approval of the study protocol must also be provided in the manuscript.

Flow Cytometry

Plots

Confirm that:

☒ The axis labels state the marker and fluorochrome used (e.g. CD4-FITC).

☒ The axis scales are clearly visible. Include numbers along axes only for bottom left plot of group (a 'group' is an analysis of identical markers).

☒ All plots are contour plots with outliers or pseudocolor plots.

☒ A numerical value for number of cells or percentage (with statistics) is provided.

Methodology

Sample preparation	All samples were washed and stained in FACS buffer (2%FBS in PBS) at 4°C
Instrument	Data were collected using a Guava EasyCyte HT flow cytometer (Millipore) or an LSR Fortessa (BD).
Software	Flow Jo software was used for all data analyses.
Cell population abundance	Typically 15,000 or more cells were acquired in the Live gate.
Gating strategy	Lymphocyes were idnetified by FSC/SSC characteristics and further refined by exclusion of doublets and DAPI+ cells.

☒ Tick this box to confirm that a figure exemplifying the gating strategy is provided in the Supplementary Information.